Ecole Polytechnique
Fédérale de Lausanne

Urban Thermodynamics

EPFL Innovation Park Microclimate Study

Autors

Mingyang Luo, SCIPER : 394972
Selina Fuchs, SCIPER : 356252
Jan Janczak, SCIPER : 357572
Garman Meyler, SCIPER : 393894
Paolina Lemaire, SCIPER : 362490

Group 10

January 10, 2025

Assist. Prof. Doolana Khovalyg

civil-309
Autumn Semester - 2024

Summary

1 Introduction **2**

2 Site Analysis **2**
2.1 Site Description . . . 2
2.2 Climate Analysis . . . 3
2.2.1 Air temperature . . . 3
2.2.2 Relative humidity . . . 4
2.2.3 Global radiation . . . 4
2.2.4 Wind Speed . . . 5
2.2.5 Thermal indices . . . 5
2.3 Modelling of Site and Simulation settings . . . 6
2.4 Neighbourhood Description and analysis . . . 7
2.4.1 General description and topographic details . . . 7
2.4.2 Comment on the Base Case Model . . . 7
2.5 Current site microclimate conditions . . . 8
2.5.1 Wind speed on the current site . . . 8
2.5.2 Relative Humidity behaviour . . . 8
2.5.3 Exposure to radiation . . . 9
2.5.4 Potential air temperature . . . 10
2.5.5 Comment on Human Thermal Comfort . . . 11

3 Urban microclimate exploration **12**
3.1 Building - environment interaction . . . 12
3.1.1 Current Situation . . . 12
3.1.2 Proposed solution . . . 13
3.1.3 Changes made to model . . . 13
3.1.4 Solution Analysis . . . 14
3.2 Ground- environment interaction . . . 14
3.2.1 Current situation . . . 14
3.2.2 Proposed solution . . . 15
3.2.3 Solution Analysis . . . 16
3.3 Water body - environment interactions . . . 17
3.3.1 Current Situation . . . 17
3.3.2 Proposed Solution . . . 17
3.3.3 Simulation results and Discussion . . . 19
3.4 Vegetation - Ground Interactions . . . 21
3.4.1 Current Challenges . . . 21
3.4.2 Mitigation Strategies . . . 21
3.4.3 Simulation Results and Comparisons . . . 23

4 Integrated Microclimate Solution **24**
4.1 Proposed UHI mitigation solution . . . 24
4.2 Analysis of the microclimate and comparison with previous proposals . . . 25
4.2.1 Absolute potential air temperature change for the different cases . . . 26
4.2.2 Absolute change in RH for the different base case . . . 27
4.2.3 Changes in Heat fluxes . . . 28
4.2.4 Comparing base cases : Overview . . . 30
4.3 Outcome of the Integrated Microclimate Solution . . . 30
4.3.1 Potential Air Temperature . . . 30
4.3.2 Relative Humidity and Wind Speed . . . 30
4.3.3 Soil Temperature . . . 31
4.3.4 Surface Heat Flux . . . 31
4.3.5 Wall and Roof Temperatures, Sensible and Latent Heat Flux of the Building . . . 32
4.3.6 PET (Physiological Equivalent Temperature) . . . 32
4.3.7 MRT (Mean Radiant Temperature) . . . 33
4.3.8 Outcome . . . 33

5 Conclusion **33**

6 Annexes **35**

7 References **36**

1 Introduction

Urban environments face increasing challenges from the Urban Heat Island (UHI) effect, causing urban areas experience elevated temperatures compared to rural regions. This issue, compounded by global warming, results in adverse impacts on human health, thermal comfort, and energy demand. Addressing these challenges requires integrating climate-sensitive design principles into urban planning to enhance resilience and sustainability. The Urban Heat

Island (UHI) effect is primarily driven by the replacement of natural surfaces with heat-retaining materials such as asphalt, concrete, and metal, which absorb and retain solar heat. Reduced vegetation cover further exacerbates the issue by limiting cooling through evapotranspiration, while heat from human activities, such as transportation and air conditioning, contributes additional warming. Urban geometry, including densely packed buildings and narrow streets, creates "urban canyons" that trap heat and restrict airflow, intensifying localized warming.

Urban microclimates, which are shaped by these interactions, play a crucial role in influencing thermal comfort, energy demand, and air quality within cities. A better understanding of these microclimates enables the development of strategies to mitigate UHI effects, such as increasing vegetation, modifying materials, and integrating water features. These approaches not only improve urban resilience but also enhance the sustainability and liveability of cities.

This project explores the microclimatic conditions of the EPFL Innovation Park, focusing on the interactions between urban elements and their effects on the local environment. Using ENVI-met, a microclimate simulation tool, future climate scenarios will be analysed to propose mitigation strategies. The report provides a detailed analysis of site conditions, thermodynamic interactions, and an integrated urban mitigation proposal.

Objectives

The project aims to:

- Critically analyse the current conditions of the EPFL Innovation Park, including land use, material properties, and climatic features, to identify hotspots and contributing factors.
- Investigate thermodynamic interactions between urban elements such as buildings, ground covers, vegetation, and water bodies, and evaluate their influence on the microclimate.
- Propose and assess integrated mitigation strategies to address urban overheating and improve thermal comfort.

Structure of the Report

The report is structured into three main components:

- **Site Analysis:** Evaluates the physical and environmental characteristics of the EPFL Innovation Park, including building materials, geometry, and green and blue infrastructure. Using ENVI-met simulations, critical hotspots and their causes will be identified, providing the foundation for mitigation strategies.
- **Urban Microclimate Exploration:** Analyzes thermodynamic interactions among various urban elements separately. Comparative scenarios assess the impacts of changing building morphology, material properties, vegetation, and water elements on the microclimate.
- **Urban Mitigation Proposal:** Develops an integrated strategy combining interventions on buildings, ground covers, vegetation, and water infrastructure. Effectiveness is assessed based on environmental parameters and thermal comfort metrics.

Methodology

The methodology combines site-specific data analysis, climate simulations using ENVI-met, and the application of urban design principles. Each phase builds upon the findings of previous analyses, culminating in an integrated mitigation proposal. Through the application of thermodynamic optimization, this project aims to mitigate the Urban Heat Island (UHI) effect.

2 Site Analysis

2.1 Site Description

The EPFL Innovation Park, located near Lake Geneva on the EPFL campus, spans approximately 11 hectares and serves as a dynamic hub for innovation and entrepreneurship. It hosts over 150 startups and the R&D units of 25 large

companies, fostering collaboration between academia and industry. The park's primary function is to bridge the gap between cutting-edge research and marketable products and services. It provides a conducive environment for startups, small and medium-sized enterprises (SMEs), and corporate research teams to thrive. Companies at the park benefit from proximity to over 500 EPFL laboratories and research centres, facilitating the exchange of ideas and technological advancements.

The campus is connected by major roads and is in proximity to public transportation options, including bus and metro lines. Within the park, the internal road network is designed to facilitate efficient movement and connectivity between buildings and facilities. Pedestrian and bicycle routes are also included to promote sustainable transportation options.

The site includes rectilinear office buildings, diverse ground covers (e.g., asphalt, concrete, soil types), and green spaces. A detailed understanding of its physical characteristics is crucial for analyzing its microclimate and proposing targeted interventions. The tables below summarize the building materials and the simulation cases analyzed during the project, which significantly influence thermal performance and mitigation strategy selection.

Layer	**Building Group A**	**Building Group B**	**Building Group C**
Facade 1	Prefabricated concrete wall (0.14 m)	Plaster (0.01 m)	Fibre cement board (0.008 m)
Facade 2	Insulation (EPS, 0.1 m)	EPS Expanded Polystyrene (0.18 m)	Sandwich panel mineral wool (0.15 m)
Facade 3	Plaster (0.047 m)	Plywood (heavyweight, 0.14 m)	Aluminium (0.002 m)
Roof 1	Gravel (0.05 m)	Gravel (0.1 m)	Gravel (0.04 m)
Roof 2	Insulation (XPS, 0.2 m)	XPS Extruded polystyrene (0.2 m)	Mineral wool insulation (0.08 m)
Roof 3	Reinforced concrete slab (0.3 m)	Concrete reinforced with steel combined with EPS insulation (0.365 m)	Reinforced concrete slab (0.35 m)

Table 1: Building facade and roof materials for EPFL Innovation Park.

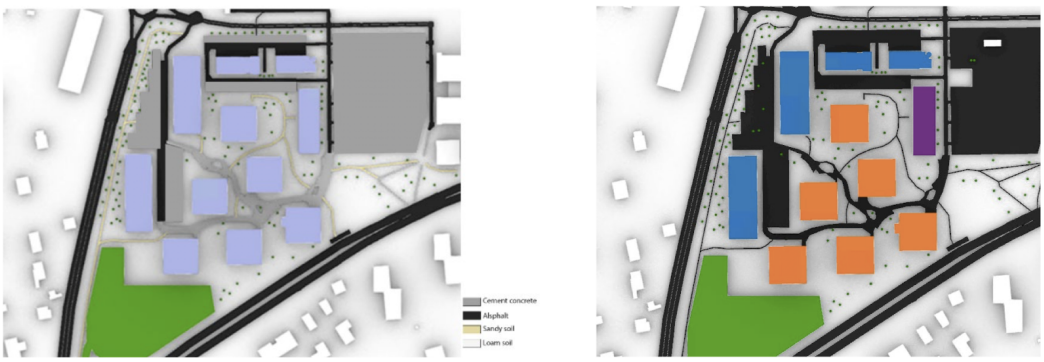

Figure 1: Details of the site: (a) ground cover, (b) building material group (See colours on table 1)

2.2 Climate Analysis

The .epw file from the nearby weather station in Esplanade is uploaded on CBE Climate tool, in order to analyse the given data as follows. The aim is to better understand the climate conditions of the Innovation Park, thanks to data collected at a nearby point on campus, Esplanade, both being similar zones.

2.2.1 Air temperature

The Lemanic region is one of the hottest of Switzerland, as it is a "marine west coast" [7]. The summers tend to be very hot and the winters are not as cold as elsewhere in Switzerland. The difference between the two seasons is significant: the mean difference between the hottest month in average, July, and the coldest one, January, is 22 °C. Over a day the hottest time is between 15h. and 16h and the coldest air temperature is early in the morning, just

before the sunrise. In summer this is around 6h and in winter it is around 7 to 8h For this survey, the hottest day was measured the 21 July with 39.4°C and the coldest temperature on 12 January and 14 February with -1.4°C.

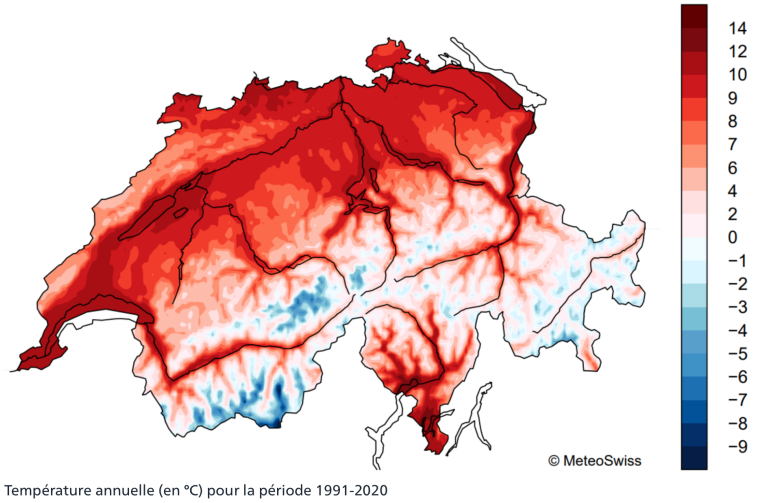

Figure 2: Mean air temperature in Switzerland

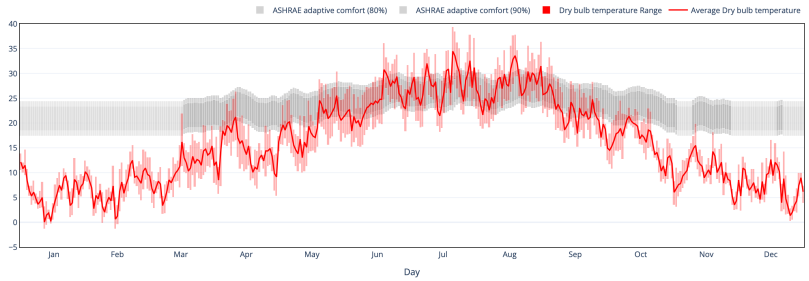

Figure 3: Dry Bulb Air Temperature on Esplanade over a year

2.2.2 Relative humidity

The site is particularly affected by humidity, which is characteristic of the Lemanic region. Over the year, the average relative humidity (RH) is at 73.83 % and during the three hottest months (June, July and August), it reaches an average of 66,6% relative Humidity, which is within the comfort zone (marked grey in figure 4). The humidity is to high to pass in the comfort band from the end of August until Mid-February, where during summer it is passes the thermal comfort check. During the winter months it is too humid for thermal comfort outside. On the other hand, during the winter months people tend to spend more time inside to escape the cold, so this fact has a reduced importance.

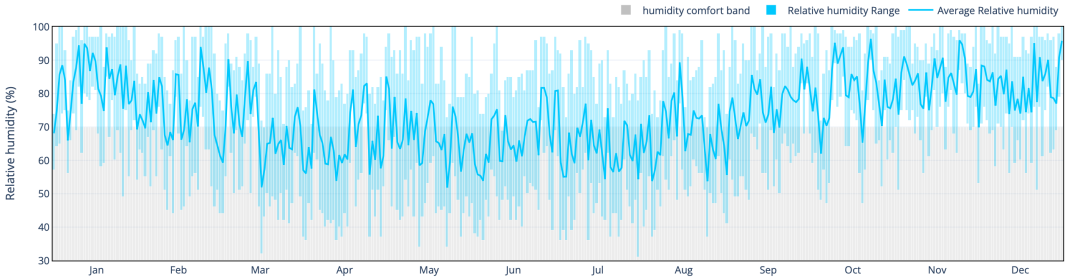

Figure 4: Relative Humidity over the year

2.2.3 Global radiation

Global horizontal radiation (GHI) is defined as the radiation received from the sun onto a horizontal surface, it is calculated as follows,

$$GHI = DHI + DNI * cos(z) \tag{1}$$

where DHI is the diffuse horizontal irradiance, the radiation from everything other than the sun on a horizontal surface, DNI is the intensity of the sunlight on a surface perpendicular to the sun rays and z is the solar zenith angle.

Global horizontal radiation and diffusion follow the distribution of sun hours over the year and the day. It is highest, when the sun shines the longest and lowest with the least sun hours. It is the most intense during noon, when the sun shines the most direct on the ground.

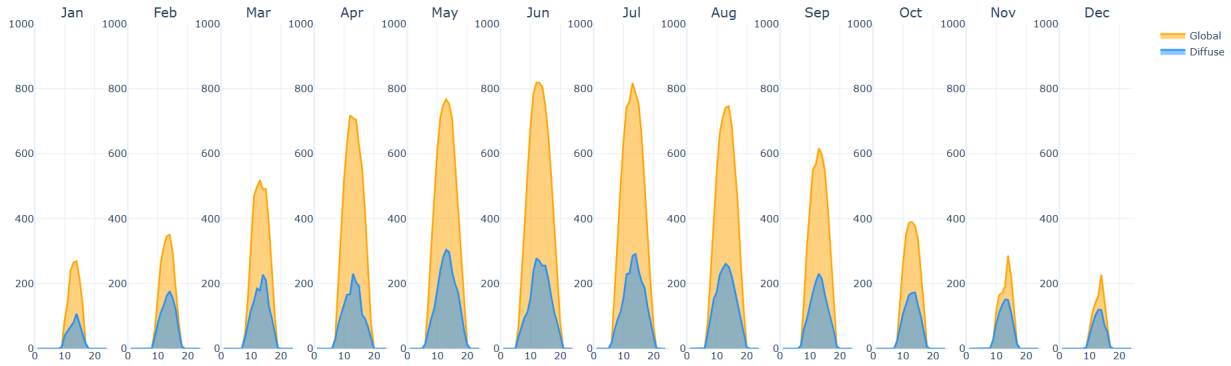

Figure 5: Global horizontal radiation and diffusion

2.2.4 Wind Speed

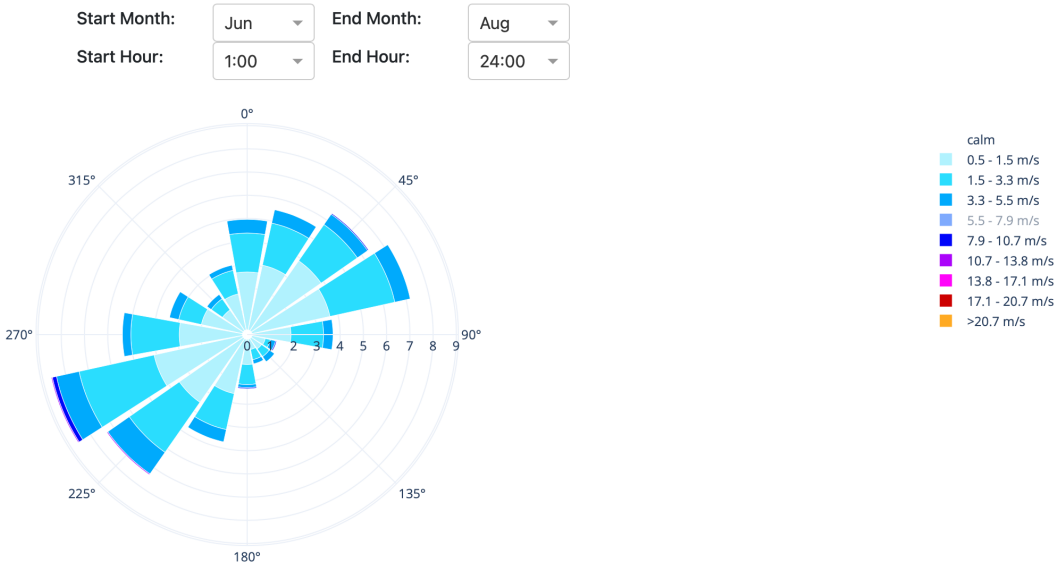

Figure 6: Summer wind rose on the Esplanade -Jun, July & August

Over the year as well as in the three hottest months, as shown in Figure 6 above, the CBE tool reveals a preferential wind direction, from the South-West direction. The opposite North-East direction is the other preferred wind direction, but with weaker intensity. In summer the wind direction shifts slightly westwards. Maximum wind speed reaches up to 13.1 m/s, but this only happened once, so it is a rare event. The mean wind speed is at 1.77 m/s during day time and at 1.37 m/s during the night.

2.2.5 Thermal indices

The aim of the site analysis is to improve the Innovation Parks urban climate. One characteristic by which this can be measured is the thermal stress indicator, which looks at the temperature from a human thermal comfort point of view.

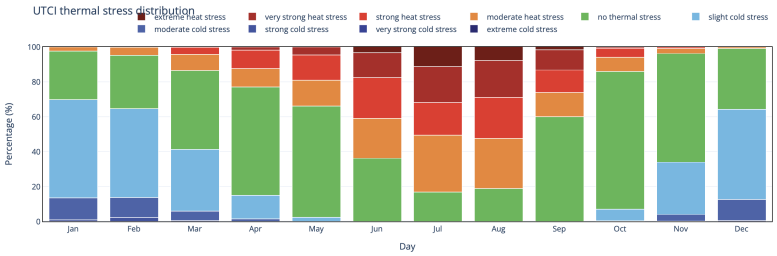

Figure 7: Esplanade thermal stress over the year

The above graph (Figure 7) provides an illustration of the days of thermal stress at the Esplanade, over the year. It shows that the area is quite impacted by heat stress, particularly in summer. For example, in July, days of heat stress constitute 83.3% of the days ; in August, it is 79.6 % of the days. Breaking the data down further, in June, 14.7 % of the days register as days with strong heat stress, up to 23.2 % in July and 22% in August. Indeed, EPFL campus in general suffers from high heat stress.

2.3 Modelling of Site and Simulation settings

The first step in making the model was creating the walls and roof of the building as outlined in the report. Although some of the materials were already present in the system, some had to be created. Their properties are outlined in the annexe, Figure 90.

Walls and Roofs can only be composed of 3 layers in ENVI-Met, as such the Roof for Building Group B had to have 2 of the layers combined into one. The concrete and EPS layers were chosen as the EPS layer had the least thickness. The combined thermal conductivity and density were computed, but the radiation properties were taken for EPS alone as this layers radiative properties would have a much larger impact being exposed to the inside of the building. The buildings were then placed with regards to the aerial photo provided.
Using both the aerial photo and photos from the site visit the ground materials were chosen. All the ground materials were defaults that were provided by ENVI-met as the testing of local ground conditions would be beyond the scope of this report. The materials used were loamy soil, for most of the ground, concrete pavement, dark for under the buildings and light for the paving, sandy loam to represent some of the paths and asphalt for the roads.

The vegetation was modelled with both 2D and 3D representations. The grass used was the $25cm$ average height preset from ENVI-met. It was not used everywhere that there was grass as an average height of $25cm$ suggests grass higher than the typical lawn present around much of the park. The bush present in the South East Corner was represented by the $2m$ high hedge preset, in line with observations from the site visit. Finally, 5 different tree types were used, varying from dense medium-sized trees mostly in the South East corner to small sparse trees dotted around the campus, as recorded during the site visit.

A weather forcing will be used with the .epw file from esplanade. Simulations will run on the hottest day, when the UHI effect is the most amplified. the 18th of August 2021 is therefore selected as the simulation day, from 06:00 for 18 hours

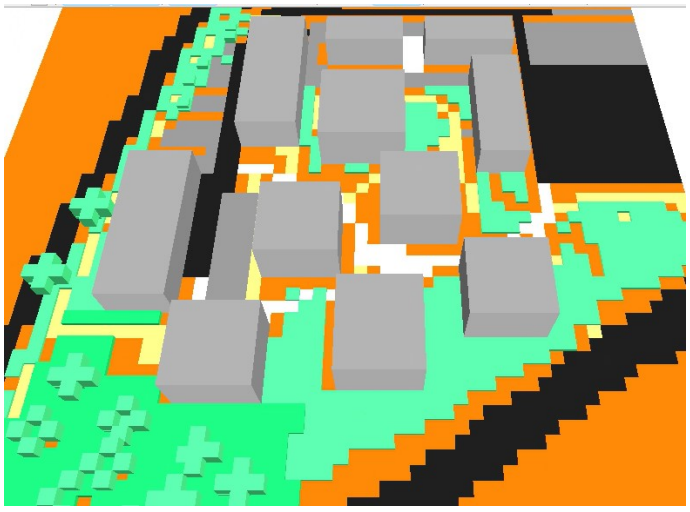

Figure 8: 3D Model used for the initial analysis

2.4 Neighbourhood Description and analysis

2.4.1 General description and topographic details

The Innovation Park neighbourhood corresponds to an LCZ5 open midrise zone, with buildings with a height of 3 to 4 floors, i.e. 10 to 15 m, separated by 15 to 25 m from each other according to the observations on site [1]. It is surrounded on its Western and Southern sides by two LCZ 6 neighbourhoods, composed of individual houses with gardens. Both zones are separated from the Innovation park by two asphalt roads. In the South-West corner of the site there is a small forest as can be see on figure 1. To the North-East is the rest of the EPFL campus, that can be characterized as a patchwork of LCZ2 and LCZ5 type zones.

The resulting canyon aspect ratio observed on the site is on average, 0.75, based on the data collected. The sky view factor, displayed on the figure 9 below, varies between 0.33 and 1.00. It can be observed on the figure below.
Another interesting point is that the Innovation park is situated mid-way between the Ecublens hill (North-west of the site) and the slope leading to the lake (South-East of the site). The Eastern facade of the hill is the first hidden from sun in the afternoon : cool air can start going down toward the lake, creating a flow from the North-West corner to the South-East corner of the site.

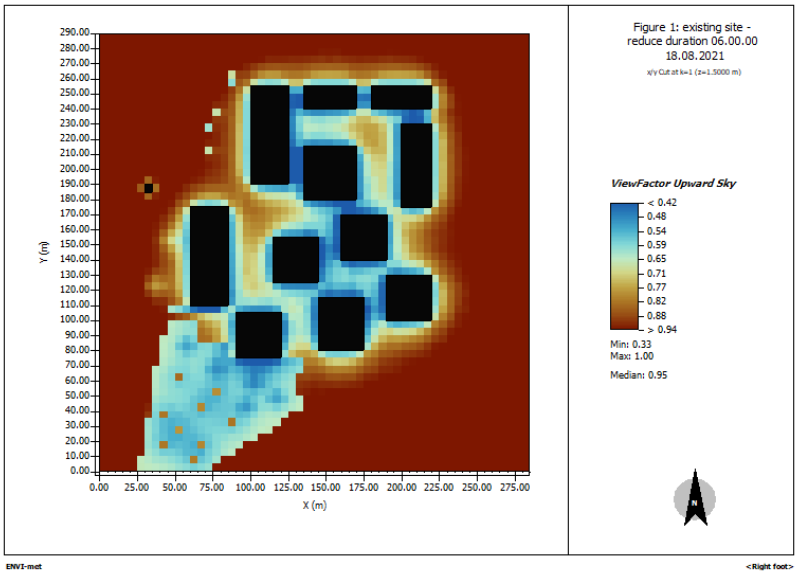

Figure 9: Sky view factor over the existing site

Figure 10: Topographic map of The Innovation Park surroundings

2.4.2 Comment on the Base Case Model

In the basecase scenario, while modelling a the point (30m,185m) was wrongly inserted as a small building of 5x5m. As the error was detected only after all simulations were done, it was decided to leave it in, but to mention it in the report as error from out part. For the interpretations as well, the region around this point will be ignored, thus some maximum or minimum values won't be taken into account because the model calculated them around this imaginary building.

2.5 Current site microclimate conditions

2.5.1 Wind speed on the current site

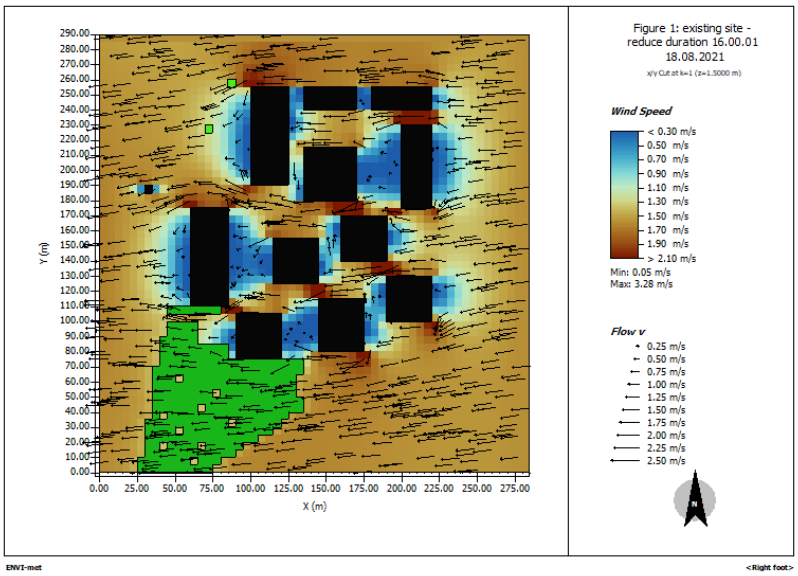

Figure 11: Innovation Park potential air temperature

As shown in Figure 11 above, the site of interest has a lower wind speed than observed on the Esplanade. This can be explained by a lower altitude and by the presence of buildings (North-East) and of the forest (South-West) that possibly reduce wind intensity from the two dominant wind directions. What can also be observed on this figure is an interesting channelling effect in-between the buildings, with the highest wind speeds observed along axis that allow wind to pass across the site, from an extremity to an other. We can in this way observe three main axis, East-West on the North part of the site, and two North/East-South/West axis, one in the middle of the site, the second on the right down corner of the Innovation Park. Each axis is corresponding to several peak wind speed points on the site. The arrows on the map, representing the fluid flows over the site, can also help in the visualisation of this channelling effect.

2.5.2 Relative Humidity behaviour

The relative humidity was plotted below at height k=1.5 m above the ground. The striking aspect is that on each map, the first one plotted for 14h and the second one for 16h, the same areas are denoting from the others. The zones with the lowest RH (Relative Humidity) correspond to the two parking lots and the two roads present in the Innovation Park, or more generally, to the areas covered with asphalt and concrete. The most humid areas, shown in lighter blue, correspond to the forest. Indeed, vegetation can help humidifying the air through its evapotranspiration process.

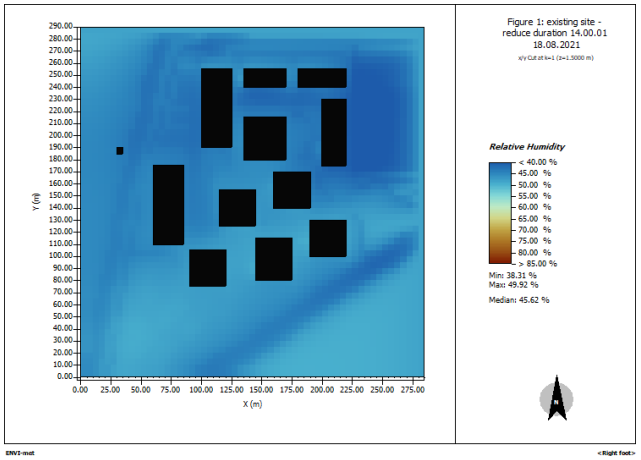

Figure 12: Relative Humidity over the existing Site - 14h

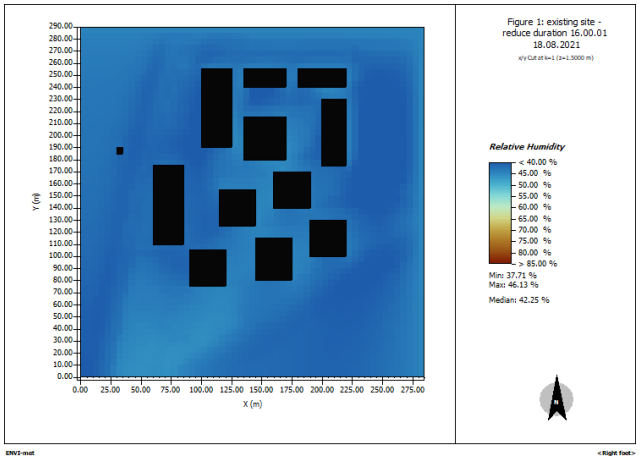

Figure 13: Relative Humidity over the existing Site - 16h

Over the entire day, RH is the highest at 8 am ; at 22h, RH is quite low due to the hot and drying summer day, but reaches up to 72.5 %. The minimum observed RH is about 37.7 %, at 16h, versus the maximum of 89.9 % reached in the morning. This maximum humidity is visible in red in the maps below.

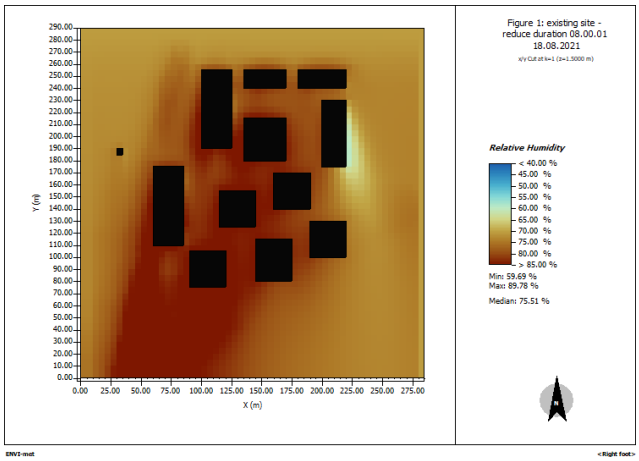

Figure 14: Relative Humidity over the existing Site - 14

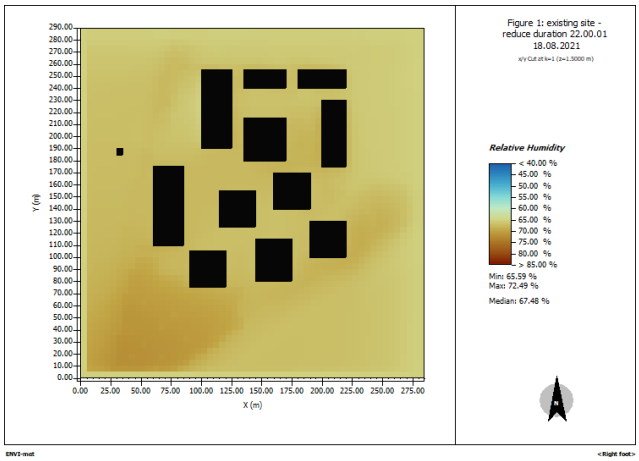

Figure 15: Relative Humidity over the existing Site - 16

2.5.3 Exposure to radiation

The Innovation Park is exposed to a lot of solar radiation, because of the little shading over the site and because of the climate. Resulting Short Wave (SW) radiation is displayed on the maps below,(Figures 16 and 17)illustrating the sum of direct, diffuse and reflected SW over the site.

The lowest cumulative SW radiations can be associated with the most shaded places on site, shown in blue and yellow on the maps below. The forest also helps in reducing SW radiation to 600.0 W/m^2. There is also a visible distinction between some zones, some are in orange and some are in more red tone. The orange ones are corresponding to the more "open" areas, i.e. the parking lots and the roads. The reddest zones, reaching up to 1538.8 W/m^2, are between the buildings. Indeed, the sum of SW radiations also takes into account the diffuse and reflected radiations, that are higher with more reflective surfaces that can reflect and concentrate them, which is the case between the buildings.

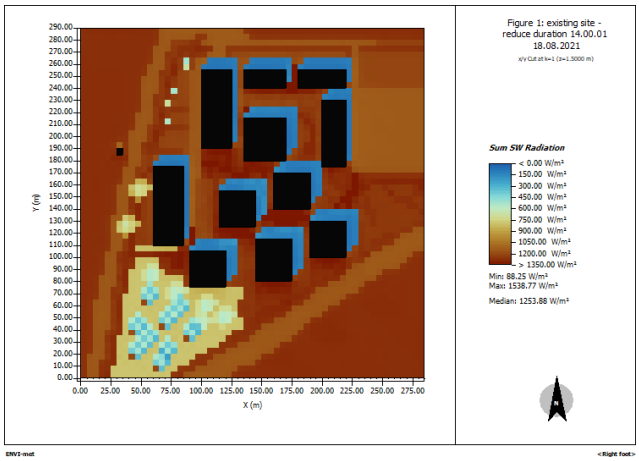

Figure 16: SW Radiation in the existing Site - 14

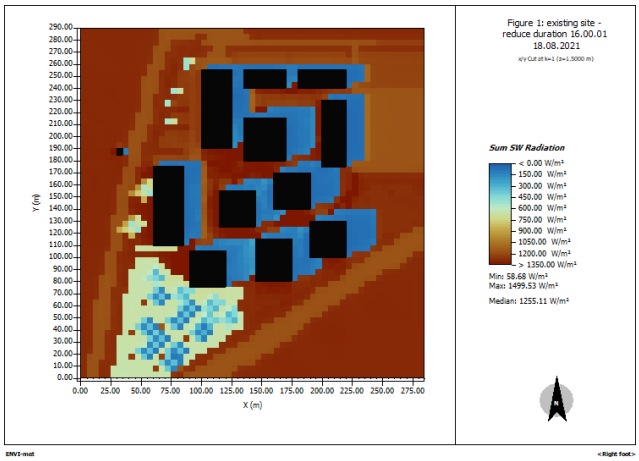

Figure 17: SW Radiation in the existing Site - 16

To detail a little more, here is a map of the radiant temperature repartition over the Site. The less irradiating surfaces can be identified as the ones hidden from sun at 14h ; their position is displayed in blue below. The forest and some other points corresponding to trees are the following least irradiative zones. What is remarkable is that some zones between the buildings are in red, reaching up to 79.1°C of mean radiant temperature. This could indicate the presence of materials storing or reflecting solar radiations on the facades, what can take part into the overall heating of the site and the buildings, by releasing energy to the surrounding environment.

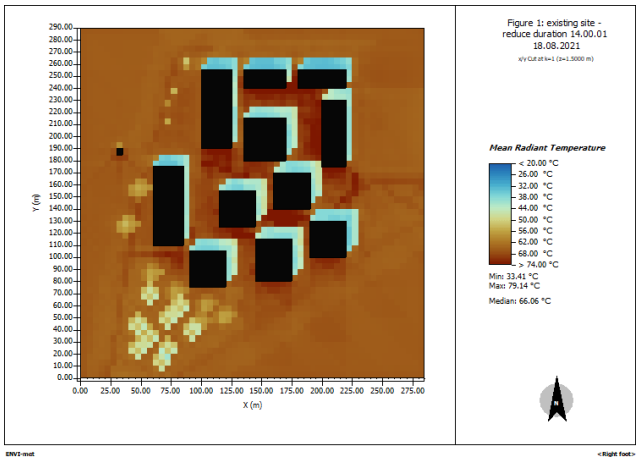

Figure 18: MRT over the existing Site - 14

2.5.4 Potential air temperature

We can observe that in current conditions, potential air temperatures in summer are higher then those at the Esplanade. Temperatures below 40.40 °C are very rare as shown in the figures below. The maximum temperature, reached at 14h, is about 43.9 °C. A jump of 4 °C is noticeable in maximum air temperature, compared to the Esplanade maximum of 39.4 °C.
Below are displayed 3 graphs that can help understand the potential air evolution between 8 and 16.

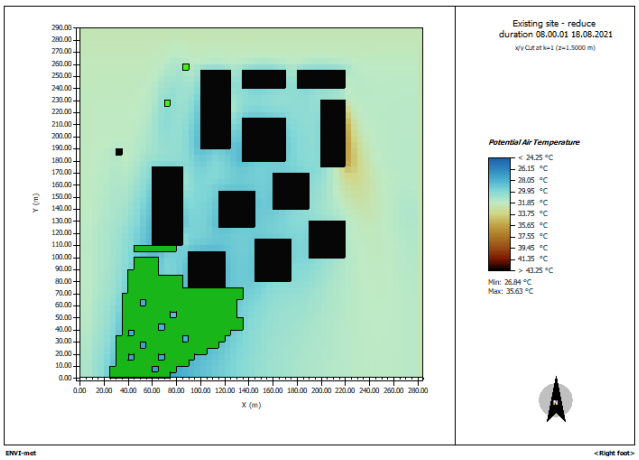

Figure 19: Potential air temperature over the site - 8h

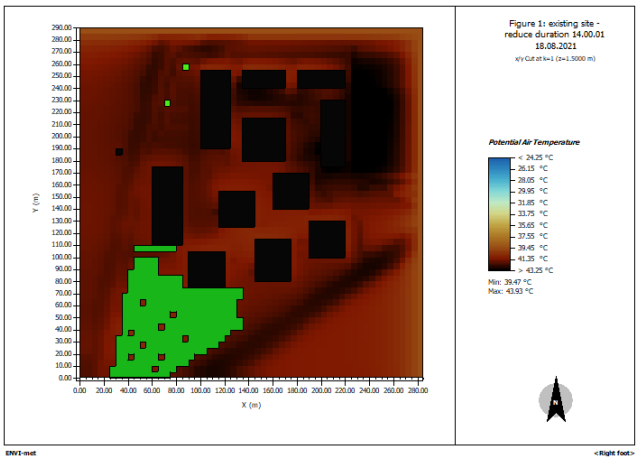

Figure 20: Potential air temperature over the site - 14h

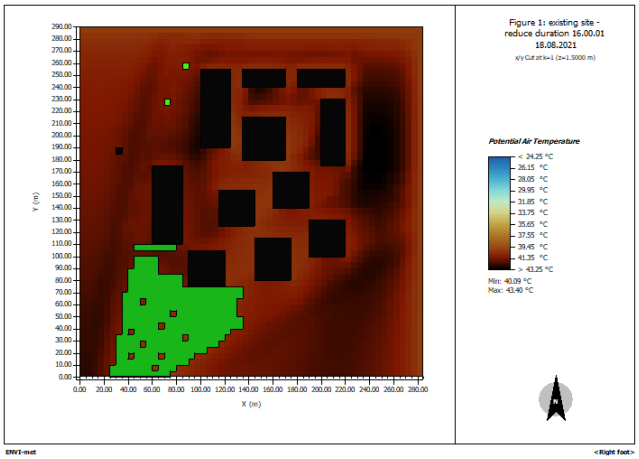

Figure 21: Potential air temperature over the site - 16h

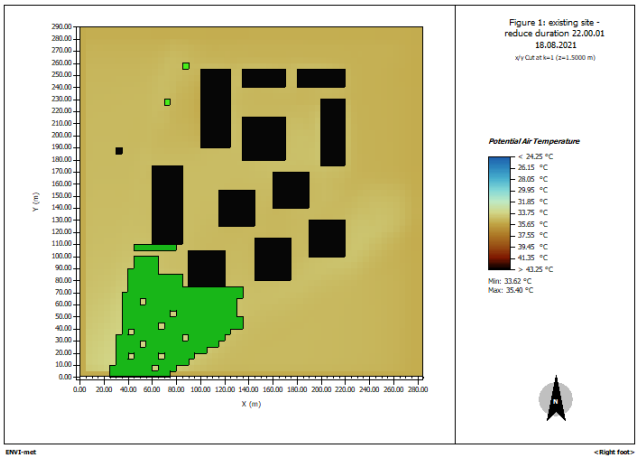

Figure 22: Potential air temperature over the site - 22h

As seen in Figure 3, in August, the maximum ASHRAE adaptive comfort at 90 % temperature is around 30 °C, temperature around which the chosen colour scale passes from light blue to light blue-green. On the figure below, it is noticeable

that these temperatures are only achieved between the buildings and in the forest : the site is already at the limit of the human comfort at 8 am. It also can be noticed that the hottest point is the eastern facade of the more eastern building, probably because it is the first facade exposed to solar radiation. There, the temperature already reaches about 34°C.

The hottest summer hours are between 12h and 16h, which were analysed in the following maps. The zones that are heating the most (in dark red below) correspond to the concrete or asphalt-covered ground. The heat in these zones radiates around, for example the heat of the road reaches the buildings southern facades. The minimum temperature is 39.5°C, which is quite high.

At 16h, the site partially begins to cool : the eastern part cools first, as can be deduced from the reduced dark area as it is less exposed to solar radiation. An hypothesis can be made that the cooling is helped by the observed fluxes from the North-west to South-East, especially because the North and west edges of the map appear as the coolest ones.

The above map (Figure 22), shows the potential air temperature after 22h, with a smaller scale, illustrating the zones that keep the highest temperatures the longest: as expected, they are the parking lots and the two roads, i.e. the asphalt and concrete zones. The other areas covered with asphalt or concrete between the buildings can be easily identified as they are highlighted in orange and red. The coolest zones, in dark and light blue, correspond to the zones covered with greenery. The forest isn't, for once, the coolest place : the forest system is indeed mitigating cooling as well as heating.

In general, throughout the day, the two parking areas and the eastern road are the hottest places on site, reaching up to 43.9°C, as can be observed in Figure 21. They also stay the hottest places at the end of the day, which can be explained by the concrete and asphalt that store heat before realising it in the evening. The coolest zones correspond to those under shade from the beginning of the day, i.e. behind the western and the northern facades. The other cooling factor being the greenery, it can be observed that the forest is also cooler, reaching potential air temperatures between 26.8°C and 39.5°C.

2.5.5 Comment on Human Thermal Comfort

The previous aspects lead to high temperatures, that make the Innovation Park a not very human-friendly environment during the summer. As seen previously, the only moment when the site achieves ASHRAE adaptive comfort temperatures is between the buildings and in the forest at 8 am, while the site is in use all day for research and innovation work, even in summer.

In the following steps, the study will focus on improvements of the current microclimate conditions, with the goal to reduce the temperatures in summer in the Innovation Park.

3 Urban microclimate exploration

Surface Energy Balance (SEB)

Before going into details, we recall first the Surface Energy Balance (SEB). It is a critical concept in urban thermodynamics that quantifies the energy fluxes at the ground's surface.

- **Radiation budget** Q^* - sum of the budget of net shortwave K^* and net longwave L^* radiation flux.
- **Sensible Heat Flux** Q_H: Heat transferred to the air above the surface through convection.
- **Latent Heat Flux** Q_E: Energy used for water evaporation from the ground.
- **Ground Heat Flux** Q_G: Heat conducted into or out of the ground's subsurface.

$$Q^* = Q_H + Q_E + Q_G \quad (\mathrm{W/m^2}) \tag{2}$$

3.1 Building - environment interaction

This section focuses on the building environment interactions, which is present in the EPFL innovation park in many ways, but most importantly in the impact of the design of the walls and roofs on the internal temperature of the buildings due to the different design of these components between buildings. This is most important as users of the campus would typically spend most of their time indoors.

It is nice to look at indoor thermal condition but the focus of this course in on outdoor conditions, the impact of buildings on the urban microclimate.

3.1.1 Current Situation

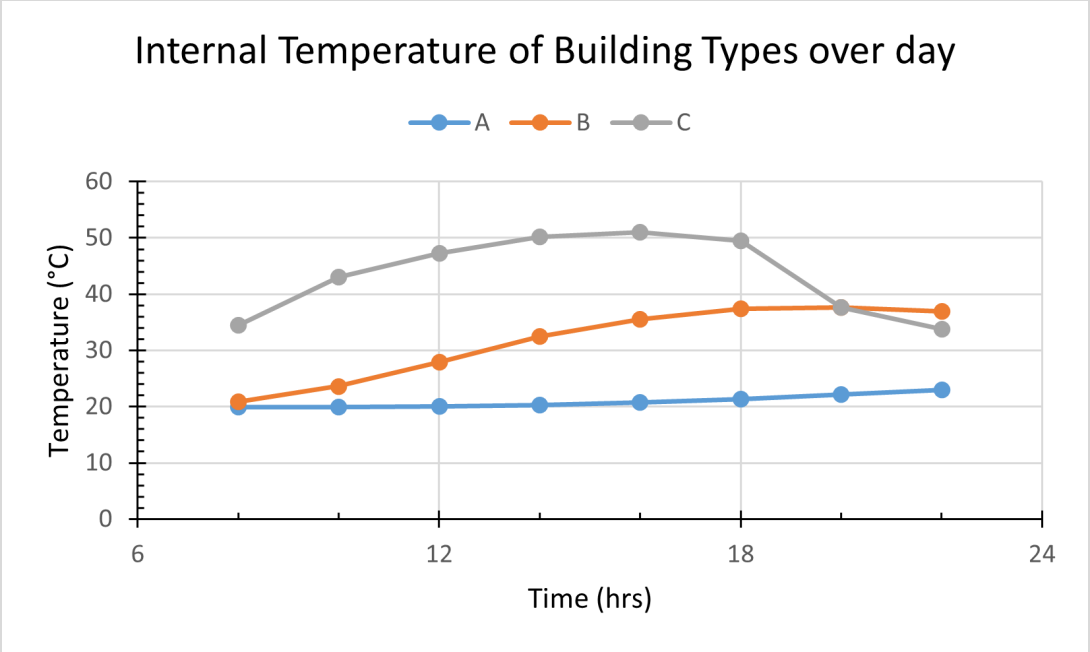

Figure 23: Internal Temperature variation in buildings

As shown above in Figure 23, Building A maintains an even temperature throughout the day around 20°C. Building B increases by 16.7°C to a high of 37.6°C at 20:00. However, the largest change in internal temperature is for Building C. It starts at an already high 34.5°C and rises 51°C at 16:00 before falling to 33.9°C a swing of 17.2°C. While there are various factors impacting this one factor that falls into the purview of this section is the sensible heat flux of the walls and roof of Building C.

The graph on figure 24 is an average of the sensible heat flux of the walls of the different buildings. As can be seen, the heat flux of Building B is quite low, explaining the increase in building temperature throughout the day as the building does not expel enough heat to prevent heating up. Building A has a larger sensible heat flux, which explains the relatively stable temperature throughout the day. Building C also has a large sensible heat flux, however this leads to a large increase and decrease in temperature throughout the day as the building's internal temperature follows that of the outside.

This suggests that Building C has a low thermal admittance, μ. Knowing this, efforts can be made to increase the thermal admittance to sequester heat in the material and to reduce the variance in internal temperature due to external temperature. The equation for thermal admittance is $\mu = \sqrt{k * C_p}$. It contains both heat capacity, C_p and, thermal conductivity k. A cursory search found that most research into insulation materials focused on the latter value, and so to improve μ it was decided to search for a material with a lower value of k.

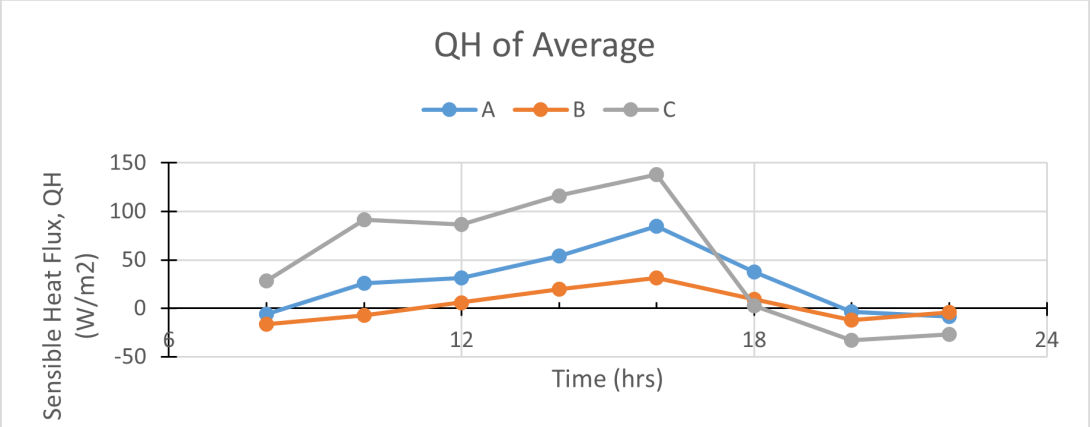

Figure 24: Average Sensible Heat Flux of all facades for different buildings

3.1.2 Proposed solution

Having considered a number of insulating materials 2, were selected. The first option was a wood cladding based on research by Yoshida, A, et al (2017) [16]. This was chosen as it had a low k-value of 0.081 W/mK and a density of 367 kg/m^3. As well, wood panelling could have better reflective properties and a certain aesthetic appeal, both other important factors. The second material chosen was a new mineral fibre insulation investigated by Moretti, E., et al (2016) [17] and now sold under the name Nobilium. This was chosen due to its low k-value of 0.0312 W/mK and a low density of 167 kg/m^3. As well, its similarity to the current mineral wool insulation was a factor as it was thought that maybe a slight improvement would bring improvement in performance.

3.1.3 Changes made to model

2 New walls were developed for Building C:

- **Option 1**: C002, consisted of 22 mm of new wood panelling, the thickness used in Yoshida, A, et al (2017) [16], 150 mm of sandwich panel mineral board, and 2 mm of aluminium. (See Fig. 26)
- **Option 2** : C003, consisted of 8 mm of fibre cement board, 150 mm of the new mineral fibre insulation, the same thickness used in the original wall, and 2 mm of aluminium. (See Fig. 27)

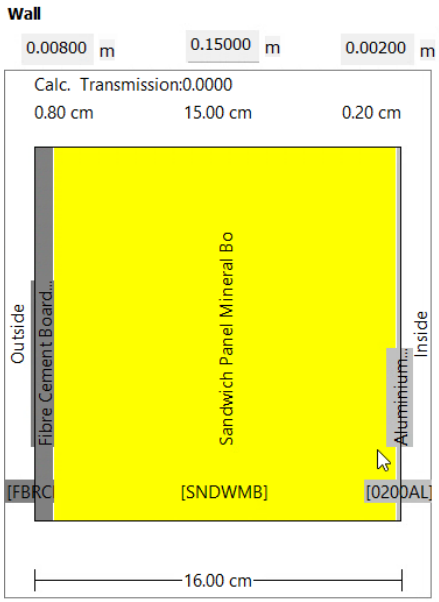

Figure 25: Cross-section of original wall, C001

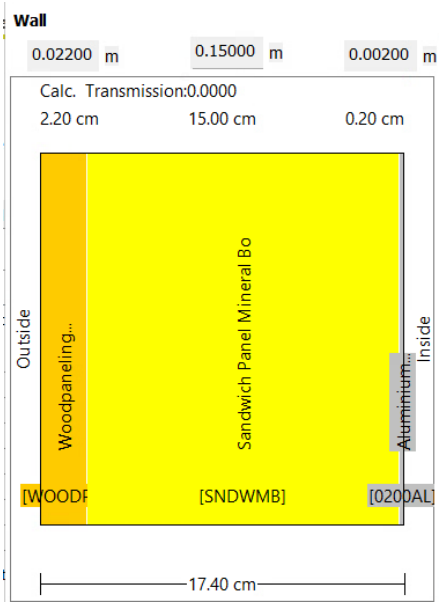

Figure 26: Cross-section of Option 1, C002

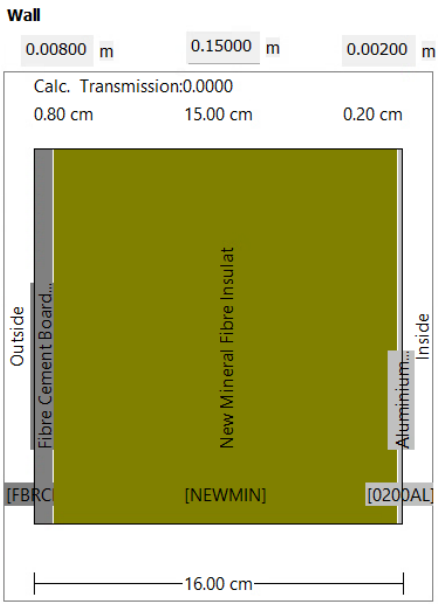

Figure 27: Cross-section of Option 2, C003

3.1.4 Solution Analysis

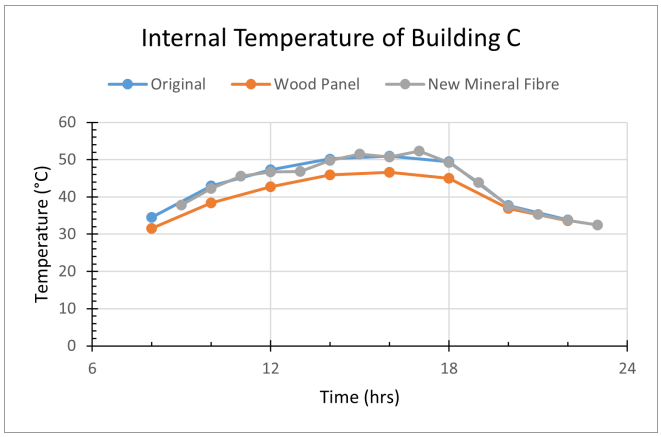

Figure 28: Comparison of internal temperature of Building C between different wall types

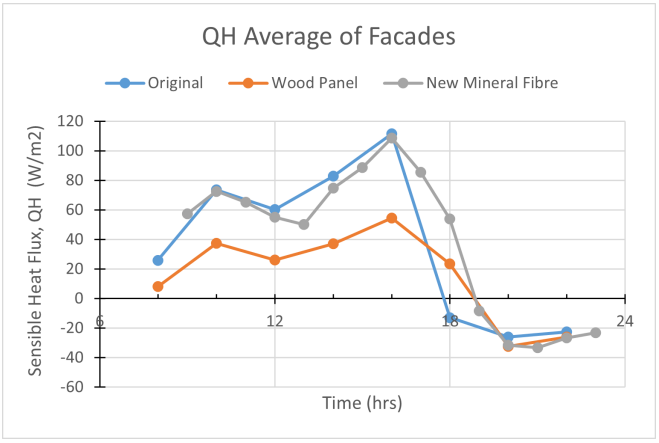

Figure 29: Comparison of sensible heat flux of Building C between different wall types

You could also look at radiative heat flux, fibre cement board and your wood panel have different albedo value, they absorb different amount of radiation.

As can be seen in Figure 28, Option 1 reduced the internal temperature of Building C by at most 4.6°C, while Option 2 had little impact. Option 1 also had a reduction in the sensible heat flux, Q_H, (Figure 29) with a maximum of $57W/m^2$ difference between the original and Option 1 at 16:00, having a lower heat flux except for at 18:00, indicating less sensible heat entering the building which goes some way in explaining the reduction in internal temperature for Option 1.

These findings suggest two things. One, wood panelling should be further investigated as it reduced the internal temperature, and two, the slight improvement in k-value for the new mineral fibre insulation did not lead to much of a change in internal temperature and as well the wood panelling had a higher k-value yet led to a greater improvement, suggesting that little can be gained in reducing the k-value.

3.2 Ground- environment interaction

This section will focus on the soil and surface interaction with the environment of the studied area. At the EPFL Innovation Park, the current ground cover includes a mix of impervious surfaces (e.g., asphalt and concrete) and natural surfaces (e.g., loam soil and vegetation). Impervious surfaces significantly alter the SEB (surface energy balance) by:

- Increasing heat absorption and storage due to low albedo and high thermal conductivity.
- Limiting evaporation because of poor water permeability.
- Enhancing the release of stored sensible heat, contributing to localized warming, especially in the evening.

3.2.1 Current situation

Figure 30 and 31 illustrate the fluctuations of various heat fluxes within the asphalt and soil of the EPFL innovation park. Notably, non-permeable surfaces, which are prevalent in the EPFL innovation park, exhibit higher temperatures due to elevated sensible heat. This phenomenon is attributed to the absence of latent heat transfer through evaporation, which is hindered on these surfaces. Consequently, the soil heat flux and sensible heat tend to be significantly higher for the asphalt compared to the soil. Furthermore, the high conductivity and heat capacity of the asphalt enable it to store more heat, which is subsequently released later in the day, further increasing the surface temperature in the evening. Figure 32 illustrates a consistent pattern. The soil temperature beneath vegetation is notably lower, as anticipated. Furthermore, the concrete surface of the building foundations effectively moderates the temperature, resulting in a cooling effect on the building, which is highly advantageous in this case.

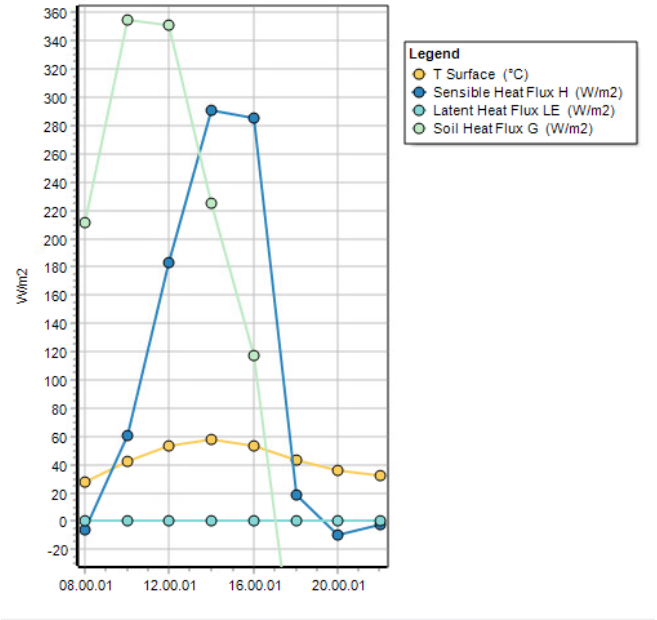

Figure 30: Heat fluxes during the day on the asphalt parking lot of the EPFL Innovation park

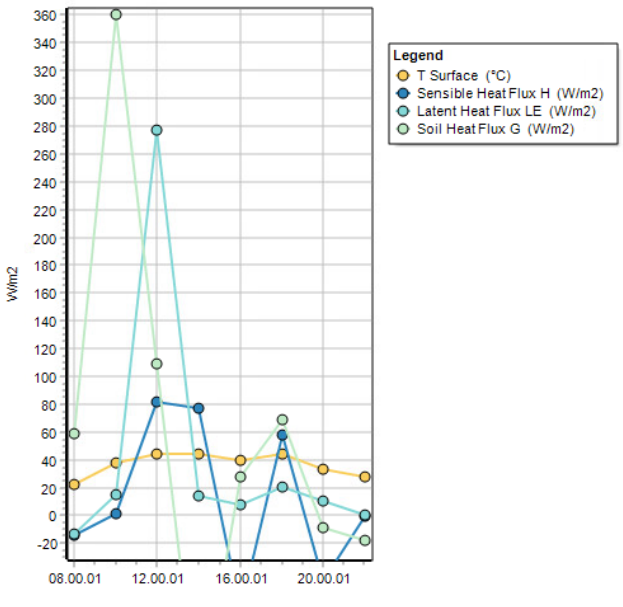

Figure 31: Heat fluxes on the soil surface next to the parking lot

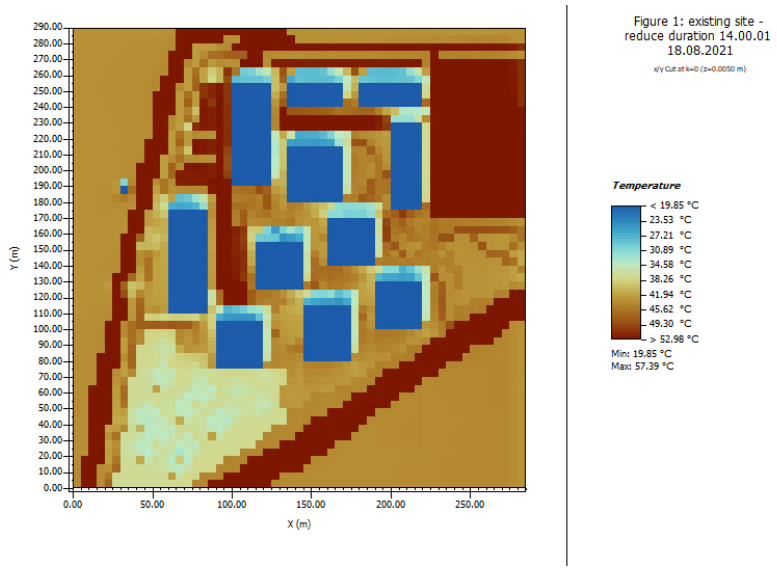

Figure 32: Soil temperature at 14h

3.2.2 Proposed solution

Key Properties that will be modified to study the ground interaction:

1. **Thermal Conductivity (k)**: Determines the rate of heat transfer through ground materials. We will try to use more natural surfaces to lower it
2. **Heat Capacity (Cp)**: Governs the amount of heat the ground can store.
3. **Albedo**: Reflectivity of the surface, influencing absorbed solar energy. We will try to put reflective coatings on pavements to lower its heat absorption. [6]
4. **Water Permeability and Moisture Content**: Affects evaporation - decreases sensible heat (Temperature) by increasing latent heat transfer, which is favourable in our case. [5]

Changes brought to the model

A few new materials were added to the ENVI-met database with reasonable changes of properties:

- Porous asphalt [3] with a reflective coating: allowing water permeability (but smaller than soil) of $1 * 10^{-6} \frac{m}{s}$ and a higher albedo of 0.35. Heat capacities and conductivity were kept as in deafult ENVI-MET materials

- Permeable light concrete [4] - same principle as porous asphalt, but with albedo of 0.5
- Dense grass of 35 cm (previously only 25cm)

With these materials, significant changes to the model are brought. All the grass on the soil will be allowed to grow higher, thus potentially impacting the evaporative cooling. Asphalt and concrete surfaces will be replaced by new porous asphalt and permeable concrete surfaces, as well as some pavements inside the campus will be just a sandy soil paths to also limit heat capacity storage.

3.2.3 Solution Analysis

Figures below present changes of the outputs from the new model compared to the base case output. We can clearly see that as anticipated, our changes brought to the model significantly change the surface temperatures, thus influencing air temperature and thermal comfort. The asphalt and concrete surfaces temperatures on the road and the parking reduced significantly at 14h, by around 12°C, and between the buildings, surface temperature of pavements was reduced by 1-2°C as seen on figure 33.

Figure 34 and 35 show the new heat flux diagrams and the change of air temperature at 14h. For the heat flux diagram, we can see well that the sensible cooling is reduced (from peak 290 W/m2 to 40 W/m2) significantly while latent heat increased (from peak 0 to 400 W/m2), which decreases our temperature as discussed before. The air temperature also reduced, especially on the parking lot by about 2.5° C. Inside the campus, the temperatures reduced by around 0.5° C. This shows our mitigation strategies to reduce the air temperature and therefore improve the thermal comfort work well as expected.

Ground Heat Flux

In this analysis we will also focus on ground heat flux, which heavily impacts the energy balance for the ground-surface interaction with the environment. Heat transfer within the ground is primarily governed by conduction.

- The ground heat flux, Q_G (measured in W/m^2), can be calculated using Fourier's Law of Conduction:

$$Q_G = -k \cdot \left(\frac{dT}{dz}\right)_{z=0} \tag{3}$$

- Alternatively, the ground heat flux, Q_G (measured in W/m^2), can be derived from the sinusoidal thermal wave equation by:

$$Q_G = \sqrt{\frac{2 \cdot \pi \cdot C_{p,s} \cdot k_s}{P}} \cdot A_s \cdot \sin\left(\frac{2\pi}{P}(t - t_m) + \frac{\pi}{4}\right) \tag{4}$$

Soil heat flux is presented on the heat fluxes charts as the bright-green curve. We can see that due to reflection of heat (high albedo materials) , the soil heat flux which stores the energy inside the ground is also decreased - from peak 360 W/m2 to 290 W/m2. This has a big impact on the UHI since the soil heat flux is usually released at night into the air, which heavily increases the temperature at night. By reducing the soil heat flux with high albedo materials, we mitigate the night UHI effect.

It is interesting to see that we indeed keep a constant radiation budget from the ENVI-met diagram, which give coherent and logical results: At Noon, Classic Asphalt: 350 + 180 + 0 W/m2 = 530 W/m2; Porous Asphalt: 290 + 200 + 25 W/m2 = 515 W/m2. The difference is negligible.

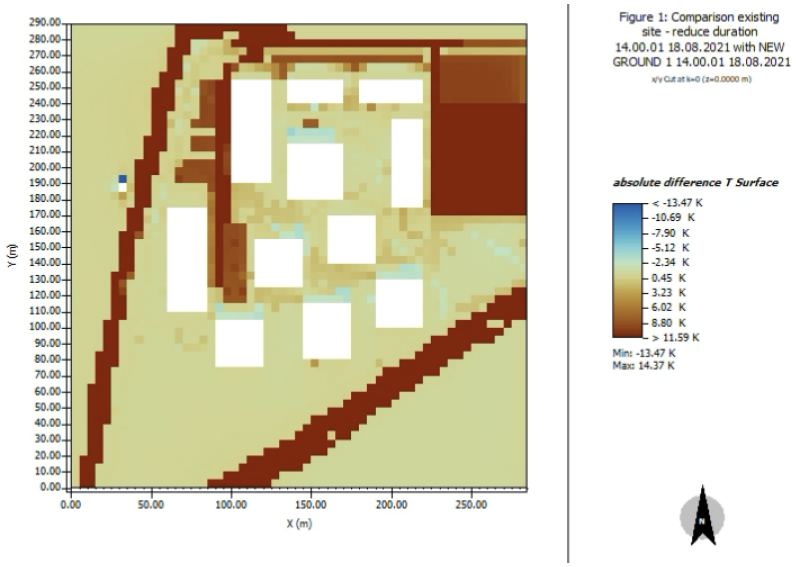

Figure 33: Soil temperature difference at 14h

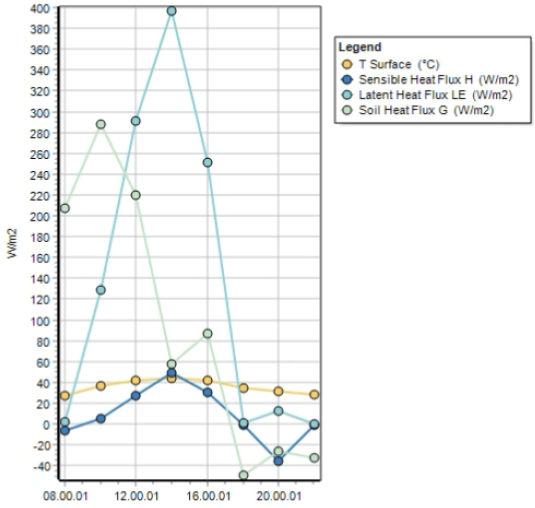

Figure 34: Heat fluxes during the day on the porous asphalt parking lot of the EPFL Innovation park

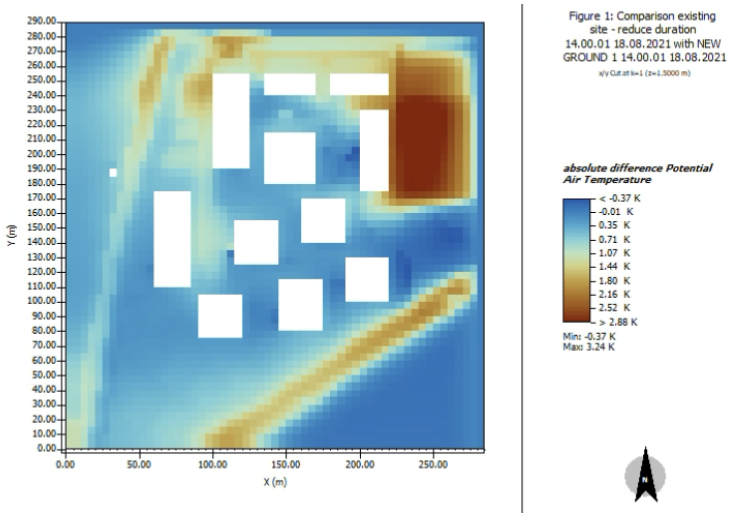

Figure 35: Air temperature at 14h

3.3 Water body - environment interactions

3.3.1 Current Situation

In the current situation, there is no open water body in the EPFL Innovation Park, however , Lake Geneva is nearby, meaning the climate is still relatively humid.

3.3.2 Proposed Solution

One of the possible solutions to reduce the temperature on site is to install ponds, fountains or water sprays. Ponds can be installed in three different positions on site:

- Between the buildings
- Between the street and the southern buildings
- Replace the forest by a biotope

The first solution decreases the temperature between buildings and does this more effectively directly around itself than if there were several small ponds [8], but is not practical because all paths would have to be destroyed and the connection between buildings would be lost. It is unknown, how the facades of the already built buildings would resist the new constant humidity.

In summer, the third solution would be very effective, because the wind could cool down over the biotope and then flow between the buildings, which requires the water surface to be free and not have any high reeds. Then the solution will accelerate the wind speed, because there are no obstacles to slow it down. Negatively impact can this solution the site in winter, where high-speed and cool winds aren't wanted between the buildings and the chronic humid air damages the building façades more easily than dryer air. And the forest has some important advantages for the site and thus, should not be removed:

- It stops the wind from entering at high speed in the park, so in case of a storm this provides protection.
- The trees help purify the air and provide shade during summer.
- They provide a source of more moist air, store water and prevent flooding due to the higher infiltration capacity of forest soil.

The second solution is a compromise for the largest possible area [8] without having to change existing features of the Innovation Park (see figure 36). Situated next to the forest[9] and between the street and the most southern buildings, it risks not to be very effective for a reduction of the heat in the heart of the park, because it is shown that the cooling effect of a pond doesn't spread further than 20m away from the water surface[9]. But it can create a good microclimate around itself, as a place to spent short breaks outside in summer. The vegetation from the forest helps keep the fresher air around the pond. This effect is also known as Urban Cooling Island effect (UCI) [1]. The surface of the pond should be dense and not too spread out over several sidearms of the pond, to better resist droughts.

Heat capacity between water and air of 3000 times is not true

The cooling effect of the pond comes from evaporative cooling, due to evaporation from the surface of the pond and due to the thermal inertia of water and high heat capacity (more than 3000 times higher than air) [1], it takes longer to heat up and to cool down, which means during the hottest phase of the day it is cooler than all its surroundings and during the early morning hours it is warmer than the environment.

Thus, for the simulation, the second solution is chosen, but accompanied by another mitigation strategy. For further cooling between the other buildings, a total of four fountains is installed. They provide moisture and a lower air temperature around them. Their positions are indicated as red rectangles in the figure 37 below.

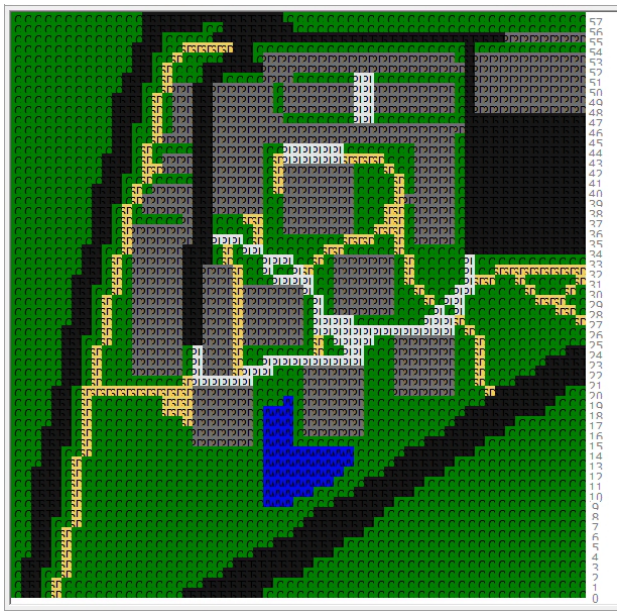

Figure 36: Position of the Pond (blue)

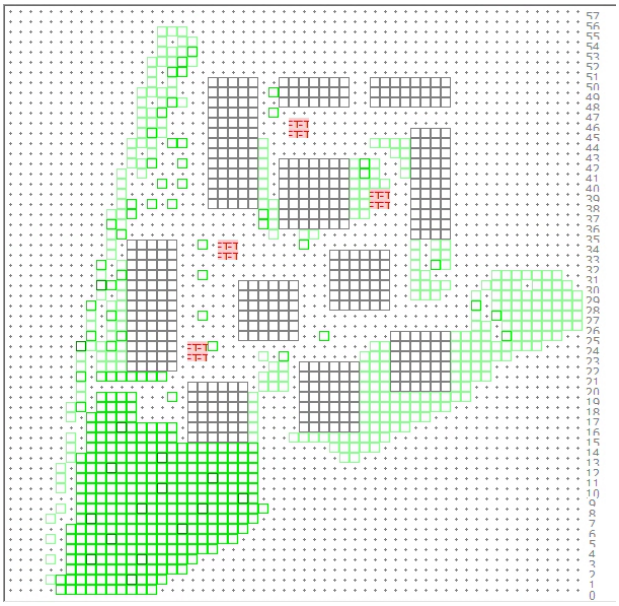

Figure 37: The Placement of the Fountains (red rectangles)

Figure 38: Overall caption for the figure

The most southern fountain is positioned in order to cool down the wind coming through the opening between the buildings, such that a larger area can be cooled with one fountain [10]. The other three fountains are placed in places where people may enjoy their break or pass when changing buildings. The two upper right fountains are located in quite narrow Street Canyons, with small wind speed and a relatively high air temperature compared to the rest of the Park, where they should decrease air temperature [11]. When observing the sun exposure of the fountains in figure 39, one sees that the fountains are all placed in areas without full sun exposure, but maximum 9 hours that day, to avoid too much loss of cooled air.

Evaporative cooling is most effective when there is solar radiation.

The cooling effect of a fountain comes from the heat exchange of the water with the air around it. Water gets heated up by radiation of the sun and evaporates. This phase change takes the energy from the environment and thus cools it down.

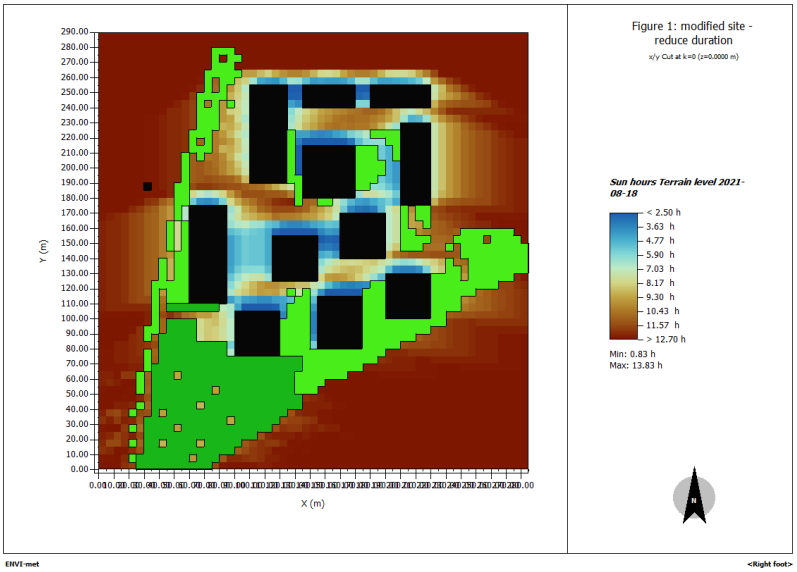

Figure 39: Cumulative hours of sun the 8/18/21

3.3.3 Simulation results and Discussion

The following figure 40 shows the potential air temperature at a height of 1.5 m over the ground at 4 p.m. in the afternoon. This is normally the hottest time over the day in summer and the height was chosen for the replication of human height, to be able to interpret the thermal comfort of the values found.

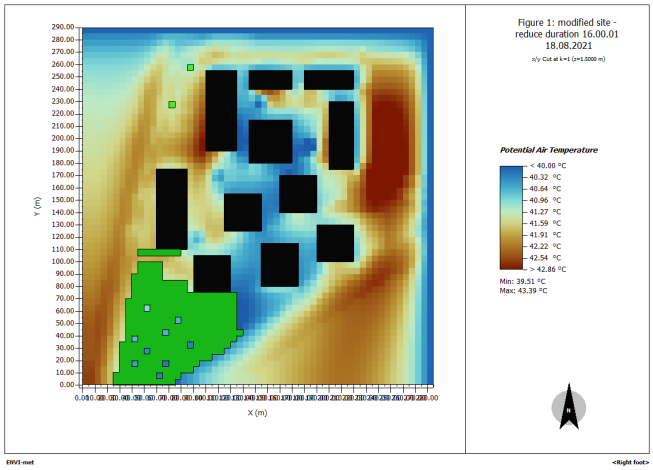

Figure 40: New Potential Air Temperature at 4 p.m.

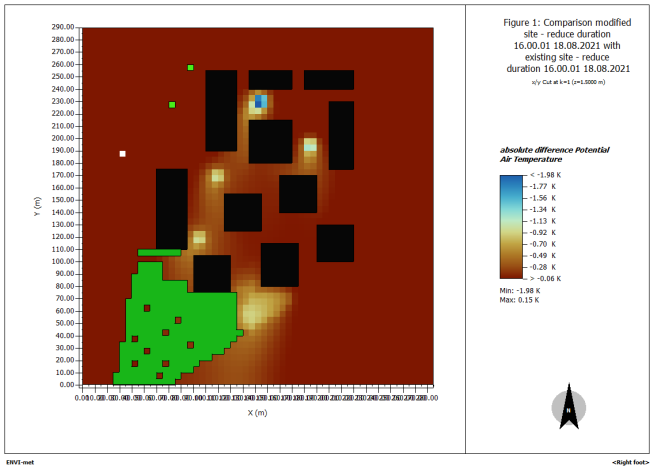

Figure 41: difference in potential air temperature

The figure 41 shows the temperature difference, the mitigation strategies have induced. The largest reduction is 1.98 K, which correlates well with the data found by Tang, L. et al (2024) [10] and to be seen for the most northern fountain, the one with the highest initial air temperature. One sees as well, that the wind direction had to be north-east, because the cooled air is further distributed in the south-west of every fountain. It is visible as well, that more than maximum 40 m away, there is no more influence from the fountain.
The figure 42 shows the very visible difference of relative Humidity the fountains make in their environment.

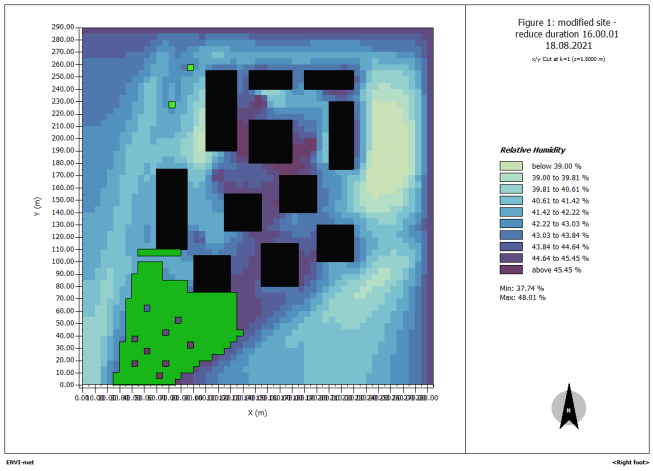

Figure 42: Relative Humidity with mitigation strategies

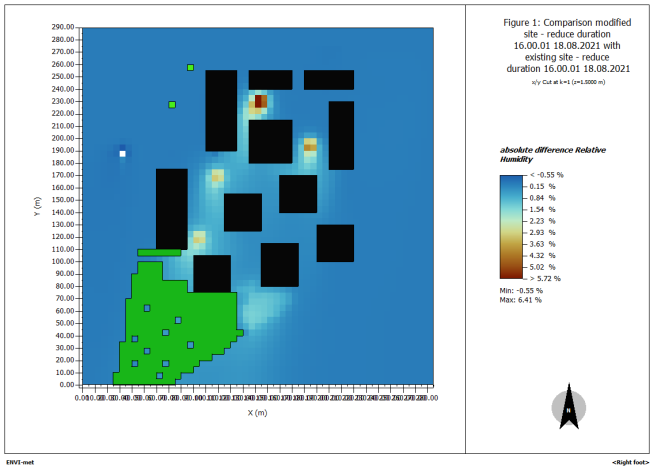

Figure 43: difference in relative Humidity

To be more precise, the figure 43 shows only the differences compared to the base case. The relative Humidity shows a similar pattern as the potential air temperature, with the highest change with an increase of 6.41% at the same fountain as the maximum air temperature change occurred. The drift of air mass towards the south-west is visible as well. Looking at the energy balance of the most northern fountain:

$$\Delta Q_S = \rho \cdot c_p \cdot h \cdot \frac{dT_{water}}{dt} \tag{5}$$

Figure 44 shows the energy balance of the most northern Fountain in the Park, Q^* and ΔQ_S have been calculated with the equation 2 for the energy balance with the addition of the ΔQ_S term 5. All the other values came directly from the simulation.

How come the latent heat flux at the fountain is 0?

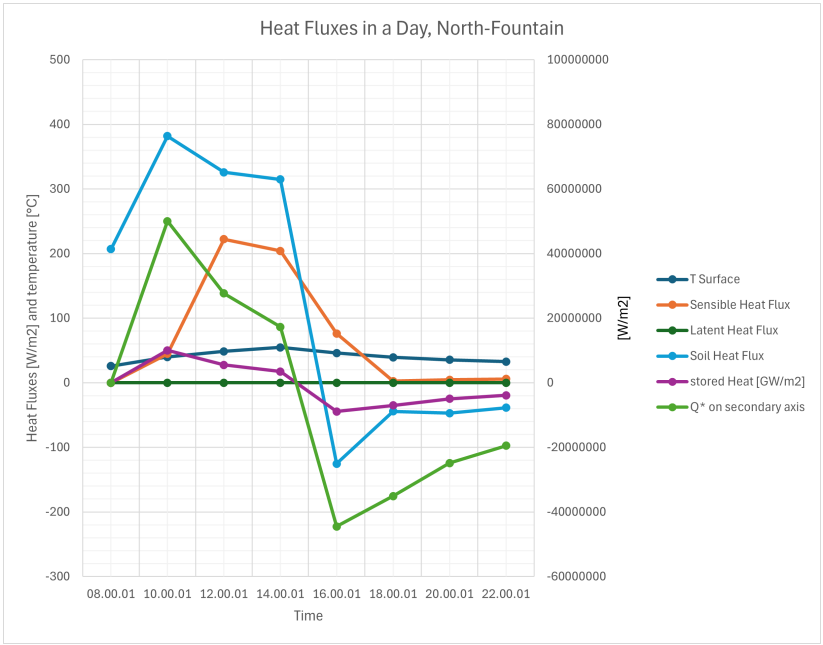

Figure 44: Heat Fluxes and Surface Temperature of the northern Fountain

As the wind is a variable hardly influenceable by water bodies, only the differences are showed in figure 45. As discussed before, it was expected that the wind speed would increase over the pond, which is visible in the graph, even though it is a very small increase, barely visible. The maximum wind change is 0.195 m/s over the pond, the lower of the two light blue points, which means that the air can accelerate slightly over the pond, as the wind flows from the top to the bottom and the lower point has a higher speed than the upper one.

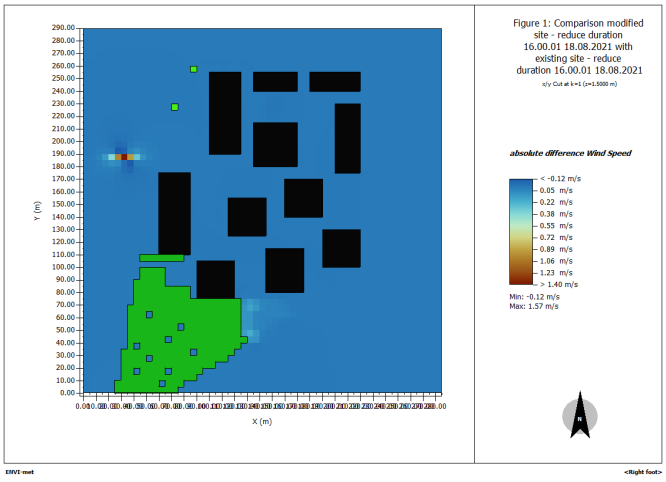

Figure 45: difference in wind speed

3.4 Vegetation - Ground Interactions

3.4.1 Current Challenges

The EPFL Innovation Park faces significant challenges related to urban overheating, particularly on rooftops, facades, parking lots, and pedestrian pathways. Building roofs exhibited extreme overheating, with maximum temperatures reaching 70°C, driven by their low albedo and high thermal mass, which caused them to store heat during the day and release it at night. This contributed significantly to the urban heat island effect and increased indoor cooling demands. The worst cases of building facades occurred in Building Block C, where facade temperatures in three directions surpassed 60°C, exacerbating indoor heat and external radiative loads. The south-facing wall of Building Block A also showed a relatively high heat concentration at around 45°C. Additionally, parking lots, especially the large lot in the upper-right corner, experienced temperatures exceeding 50°C. These large areas of exposed asphalt and concrete created hotspots that radiated heat into the surrounding environment.

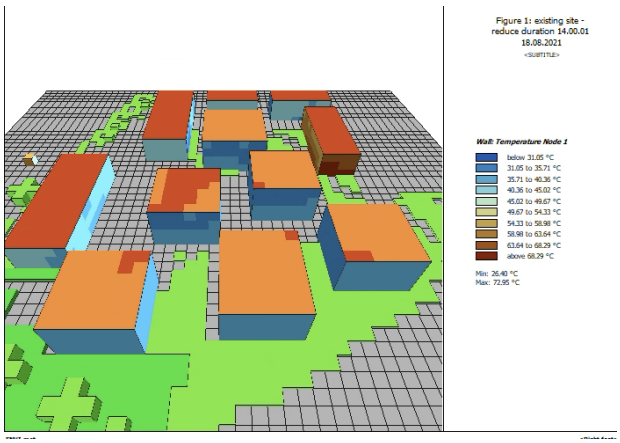

Figure 46: Wall temperature of base case at 14h.

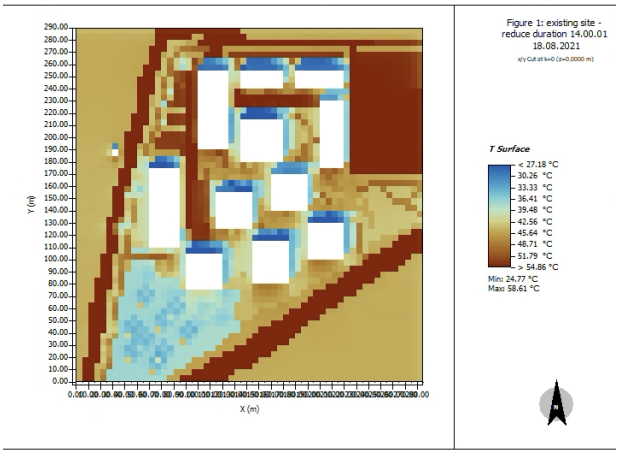

Figure 47: Surface temperature of base case at 14h.

Air temperatures in areas with insufficient vegetation reached a maximum of 44.3°C, while pedestrian pathways and streets exposed to direct solar radiation without shading recorded Mean Radiant Temperatures (MRT) exceeding 70°C, indicating severe thermal discomfort. These findings underscore a critical imbalance in the site's energy dynamics, driven by excessive solar radiation absorption, limited latent heat flux from vegetation, and dominant sensible heat transfer to the surrounding air.

3.4.2 Mitigation Strategies

Street Trees were planted systematically along major and minor roads, as well as around the perimeters and rows of parking lots. Large-canopy species, such as London Plane, were chosen for their ability to shade extensive areas, particularly along main roads. Medium-canopy species like Field Maple were used for rows and perimeters of parking lots, and Small-leaved Lime, known for its dense foliage, was planted along narrower pathways and pedestrian lanes. The cooling effect of street trees was achieved through shading, which blocked incoming solar radiation and reduced

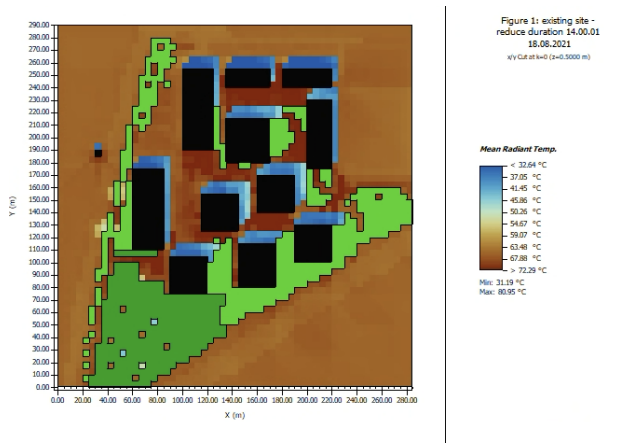

Figure 48: Mean Radiant Temperature (MRT) of base case at 14h.

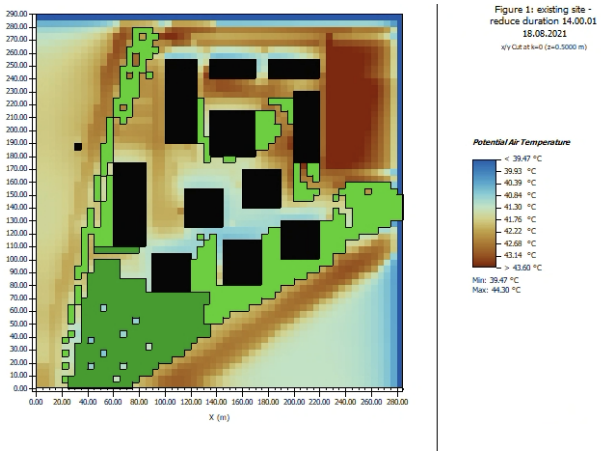

Figure 49: Potential air temperature of base case at 14h.

surface heat absorption, and evapotranspiration, which increased latent heat flux and cooled surrounding air [12, 13]. For detailed characteristics of tree species, please refer to Annex 2.

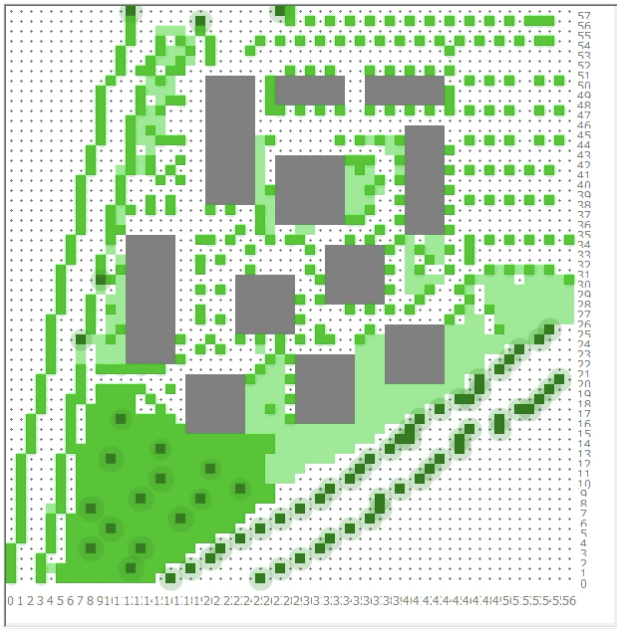

Figure 50: 2D View of Vegetation Mitigation Solutions

Green Roofs were implemented across building blocks based on structural constraints and material properties. For Building Group A, which featured heavy concrete roofs, extensive green roofs with grass (Grass 25 cm) were applied due to their lightweight nature and effective cooling potential. Building Group B, with gravel roofs, adopted intensive green roofs using Grass 50 cm, which provided deeper substrates for enhanced insulation and heat reduction. For Building Group C, characterized by lightweight aluminum roofs, lightweight green roofs with Ferns were implemented, balancing structural limitations with cooling efficiency. Green roofs reduced rooftop temperatures by increasing latent heat flux through evapotranspiration, lowering sensible heat flux, and acting as thermal insulators to minimize heat transfer into buildings [14]. Detailed parameters of green roofs are provided in Annex 3.

Green Facades were designed according to the material properties of each building block. The same vegetation was planted on three facades (south, east, and west) of each building within a block. For Building Group A, which had concrete facades, Ivy was chosen for its dense foliage and fast growth, providing effective shading and cooling. For Building Group B, with gravel facades, Funkia was applied due to its adaptability and aesthetic value. For Building Group C, with lightweight aluminum facades, Ferns were selected for their lightweight properties and effective transpiration cooling. Green facades reduced wall temperatures by providing shade and increasing latent heat flux through transpiration, while also decreasing longwave radiation at night [15]. The detailed parameters of green facades are listed in Annex 4.

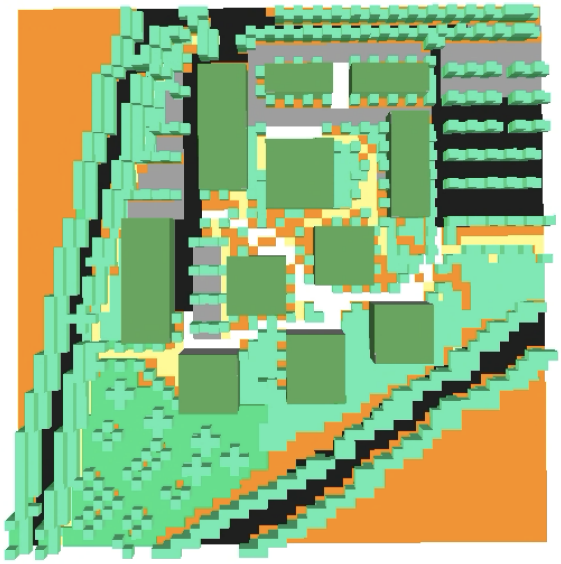

Figure 51: 3D View of Vegetation Mitigation Solutions

3.4.3 Simulation Results and Comparisons

Roof temperatures, which reached a maximum of 70°C in the base case, were reduced to as low as 30°C with the implementation of green roofs, representing a prominent cooling effect of up to 40°C. This was attributed to the insulating properties of the vegetation and the increased latent heat flux (LE) from evapotranspiration, which offset heat absorption. Previously, in the absence of green roofs, latent heat flux was nearly zero, as there was no vegetation to facilitate evapotranspiration. However, with the addition of green roofs, latent heat flux values increased significantly, as shown in Figure 53, where maximum LE values reached up to 369.69 W/m^2. This indicates a substantial increase in moisture release into the atmosphere, leading to efficient cooling of roof surfaces and reduced sensible heat flux, further mitigating urban overheating effects.

Parking lot and roads temperatures also improved significantly, with tree shading reducing surface temperatures by up to 26°C, bringing the average temperature down from 50°C to below 43°C. The rows of trees disrupted the heat-retaining properties of asphalt, minimizing localized heat accumulation and improving thermal comfort for pedestrians and vehicles.

Mean Radiant Temperature (MRT), which combines the effects of air temperature, surface heating, and solar radiation, dropped by 5–7°C in pedestrian pathways and other shaded areas. The most pronounced improvements were observed under tree canopies and near vegetated facades, where shading and transpiration worked together to improve thermal comfort.

However, the implementation of green facades demonstrated mixed effectiveness across the buildings. Building Block C exhibited the most significant temperature reductions, with the south and west-facing walls showing decreases of 25–30°C and the north and east-facing walls reducing by around 12°C. In contrast, Building Blocks A and B showed only minor reductions across most wall orientations, with the exception of Block A's south-facing wall, which achieved a 10°C reduction. These differences could be explained by the material properties of the building groups. Block C's lightweight materials, such as aluminum and fiber cement board, are highly responsive to greening interventions due to their low thermal mass, which allows for faster cooling. In contrast, Blocks A and B use high thermal mass materials, such as prefabricated concrete and heavyweight plywood, which absorb and retain heat, reducing the apparent effectiveness of green facades. Additionally, shading or less exposure to direct sunlight may have further limited the impact on these blocks. Thus, the analysis revealed that green facades bring less pronounced benefits for Building Blocks A and B. In contrast, for Building Block C, green facades proved to be a highly effective solution, significantly mitigating overheating on the most exposed walls.

Based on the results, vegetation plays a significant role in mitigating urban heat island effects. Through shading, evapotranspiration, and thermal insulation, these strategies addressed key areas of heat accumulation, such as rooftops, parking lots, and roads, while improving outdoor thermal comfort.

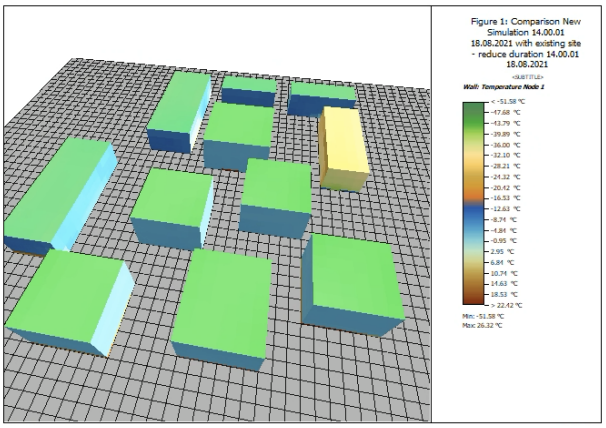

Figure 52: Absolute difference in Wall Temperature at 14h

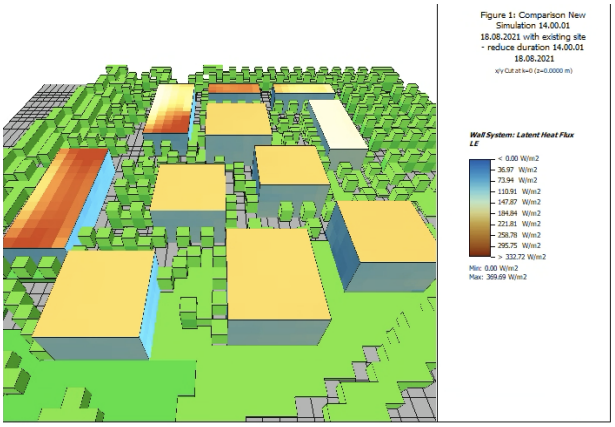

Figure 53: Latent Heat Flux (LE) at 14h

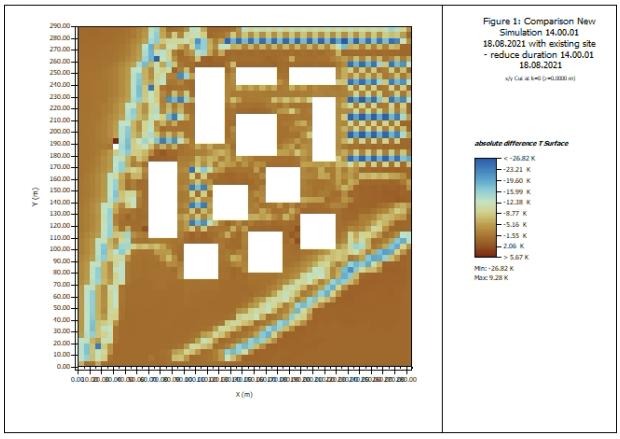

Figure 54: Absolute difference in Surface Temperature at 14h

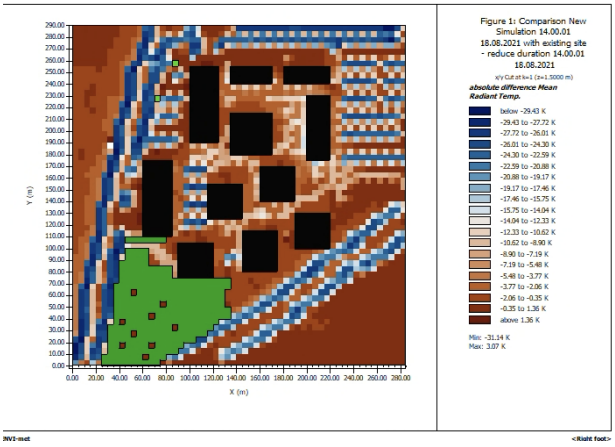

Figure 55: Absolute difference in Mean Radiant Temperature (MRT) at 14h

4 Integrated Microclimate Solution

4.1 Proposed UHI mitigation solution

In this section, we will propose an integrated solution to combat the UHI effect at the EPFL Innovation Park. The integrated model that will be simulated in ENVIMET consists of selected ranges of changes that were used and explained more in depth in the section before on individual modifications.

Changes brought to the model

- Ground interaction: We will keep all the solutions from the previous section on ground interaction: mainly the porous and permeable asphalt with reflective coatings as well as higher and denser grass coverage on the site. They all seem to be very effective in reducing temperatures especially on the parking lot. Replacing the asphalt and concrete surfaces might be expensive however, but not unreasonable as well. In fact it also does not affect at all how the space of the Innovation park is utilized.
- Building interaction: The decision was made to add wood panelling on the outside of the buildings, based on the research by Yoshida, A, et al (2017) [16] so as to reduce internal temperatures. This was chosen as reducing internal temperatures would most improve thermal comfort from a building environment interaction perspective, and the wood panelling performed much better then the other alternative which was a new mineral wool insulation developed by Moretti, E., et al (2016) [17].
- Water bodies: As seen in the previous analysis, the fountains brought the best results to the model, so it was decided to put a total of seven fountains, to replace the pond that showed smaller improvements. As seen previously the fountains haven't had a very broad influence and thus in every courtyard a fountain is placed.
- Vegetation: We adopted roof greenings across buildings, due to its remarkable impact on roof cooling. Street trees were also included in our integrated solutions, while we optimised their placement and the density to make

them more effective. Facade greenings were abandoned because they has limited effectiveness in reducing heat for Building Blocks A and B, and wall overheating was less critical in these blocks. For Building Block C, where wall overheating was more significant, we chose to add wood panelling instead of using facade greening for a better cooling result.

Figure 56 shows the final 2D model from ENVIMET Spaces. Figure 57 shows its 3D version with soil surfaces marked on the ground.

Figure 56: 2D Map of the vegetation and building layout

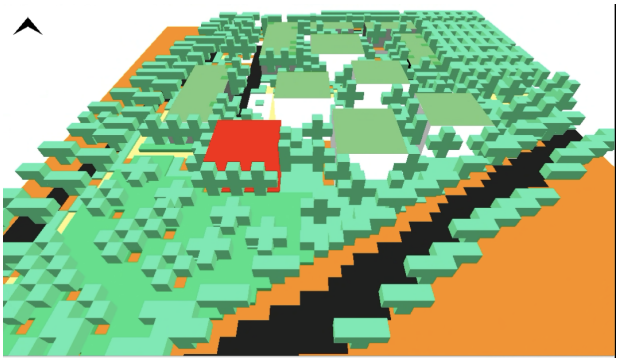

Figure 57: 3D illustration of the final model

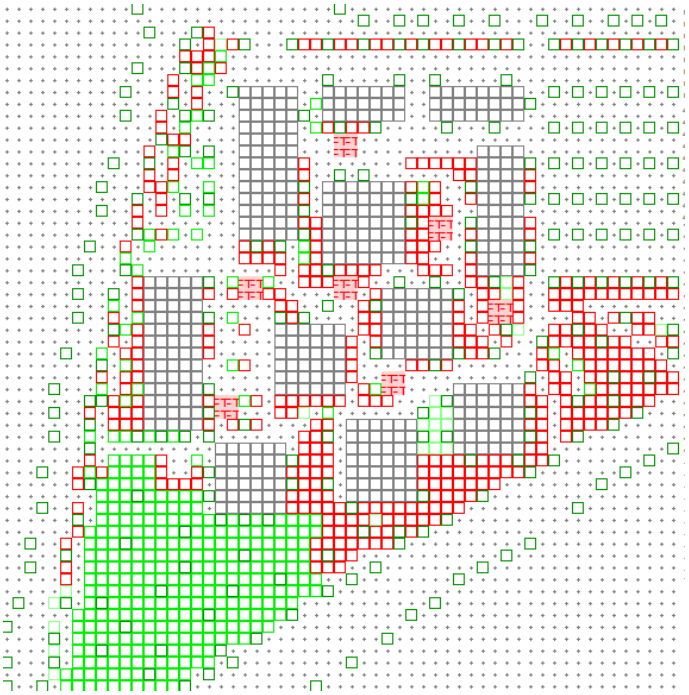

Figure 58: 2D Map with the fountains (BIG red rectangles)

4.2 Analysis of the microclimate and comparison with previous proposals

This section of the report will tackle the comparative analysis of all for base cases that were previously explored, through the spectrum of key aspects such as potential air temperature, relative humidity, latent and sensible heat fluxes and the total short wave radiations. The values for 14h were used, as this hour of the day appears as the hottest and hence, the most strategical to perform the quality of the site's microclimate. The wind wasn't considered as a key value, since no changes were brought to the occurring wind speed in any of the studied base cases, even after implementation of vegetation.

4.2.1 Absolute potential air temperature change for the different cases

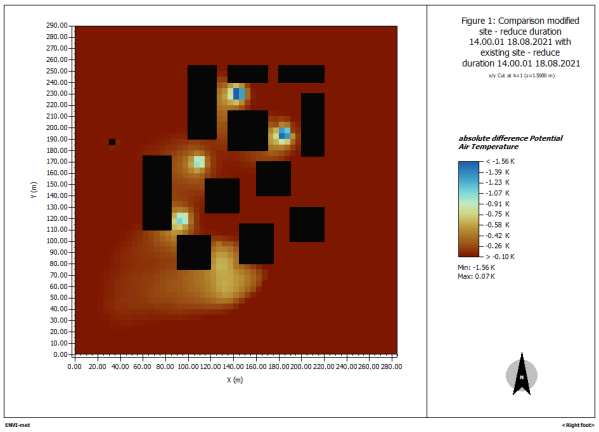

Figure 59: Potential Air temperature change with water bodies addition - 14h

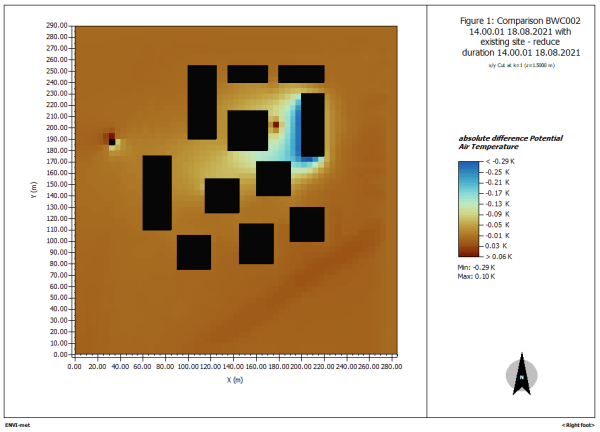

Figure 60: Potential Air temperature change with new buildings materials - 14h

For the case where water bodies are added, the humidification - as it will be seen in the next section- and related cooling effect of water bodies are very limited spatially to the close neighbourhood of the fountains. The effect of the pond is even more negligible, as mentioned before, perhaps because its effects are drowned into the effects provided by the nearby forest. The only noticeable effect is a reduced SW sum above the pound. The SW sum between the building is almost unchanged compared to the initial state. However, these water bodies can provide cooler places, out of the hottest hours that are 14h and 16h, than the rest of the site, what can make of them dedicated places for outdoor stay, in the logic of adaptative behaviour.

As for the change of Building materials, it introduces a potential air temperature decrease in a range of 0.01 to 0.1 °C, and even causes two local points with 0.1 °C more than for the existing site. The overall effects of the building material changes are therefore neglectible. The interesting effect of the green facade is on the contrary decreasing the temperatures from 0.17 to 0.29 °C locally at the place of implementation : if this solution could be implemented over the whole site, it could bring noticeable improvements between the buildings by the interaction between green surfaces.

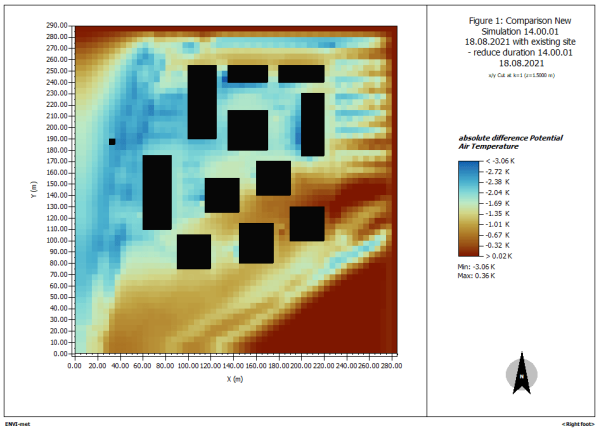

Figure 61: Potential Air temperature change vegetation addition - 14h

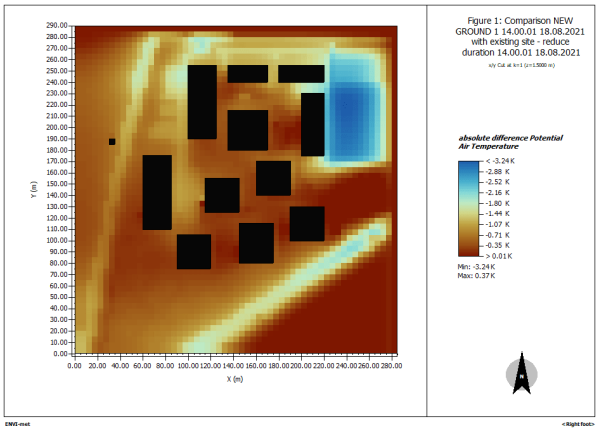

Figure 62: Potential Air temperature change with ground change - 14h

This two solutions, with added vegetation and changed ground, are bringing striking improvements over the whole neighbourhood.

Indeed, an important potential air temperature reduction can be noticed, down to 3.6 °C. Few zones are bearing a little temperature increase, but they are not within the hottest ones in the initial site. On the contrary, the initially hottest zones (the parking areas and the roads) are now significantly cooler. The higher temperature reached in the day is now 42.6°, in alternated bands on the eastern parking area, thanks to the shadow brought there by ranks of vegetation. Overall, extending the existing forest and adding greenings brings significant improvement all over the Innovation Park.

With the proposed ground change, most of the peak heat zones reduced their temperature : compared to the initial state, the simulation shows that in the hottest hours, the temperatures reached are now in the range of 39.4 to 43.3 °C,

versus the initial 39.5°C to 43.9°C. The site also appears to cool faster, indeed, at 16h, the maximum temperature is already down to 42.4°C, while in the initial site, temperatures were situated between 40.1 and 43.4. The maximum temperature reached is reduced by 1°C, and the overall result is satisfying, as it brings down most of the zones to temperatures below 40°C.

Maximum and overall temperatures are still really high but the change of ground brings visible improvements in the hottest hours of a summer day, improvements equally distributed over the site. Changing the ground also helps reducing temperatures all over the day ; the site also cools down faster in the afternoon, reaching this way much more human-friendly temperatures at the end and beginning of the day.

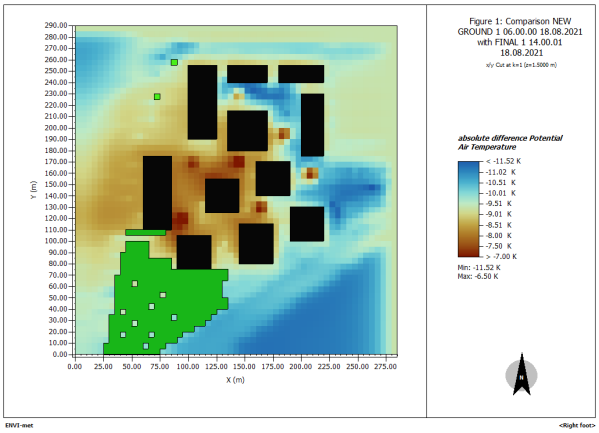

Figure 63: Potential Air temperature with ground change versus integrated solutions - 14h

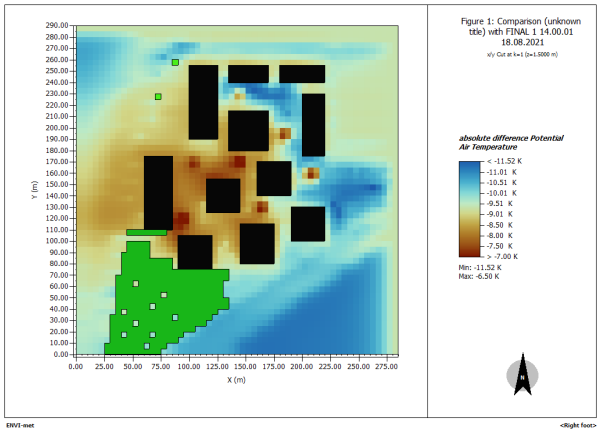

Figure 64: Potential Air temperature change with extended vegetation versus integrated solutions - 14h

As it can be seen in figures above, combining solutions helps reducing temperature all over the site. The two most impacting solutions - vegetation and ground changes- were here compared to their final effect : the ground and vegetation changes separate effects don't seem to reach the South-Eastern and the North-Western sides of the site, indeed, with the final integrated solutions, a drop down to -11.5 °C can be observed in those zones. As a result, it can be concluded that cumulative measures can have more effects than even taking only one most effective measure alone.

4.2.2 Absolute change in RH for the different base case

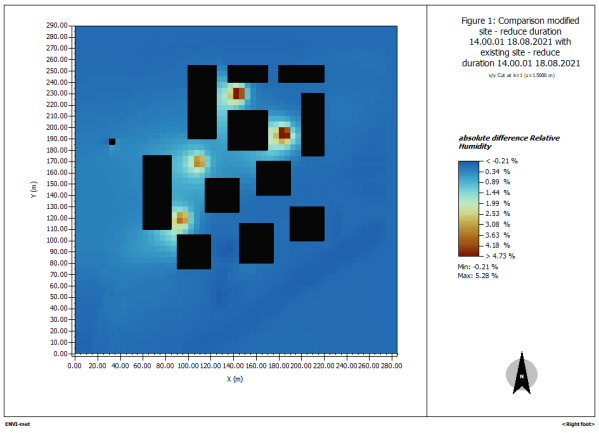

Figure 65: Relative humidity change with addition of water bodies - 14h

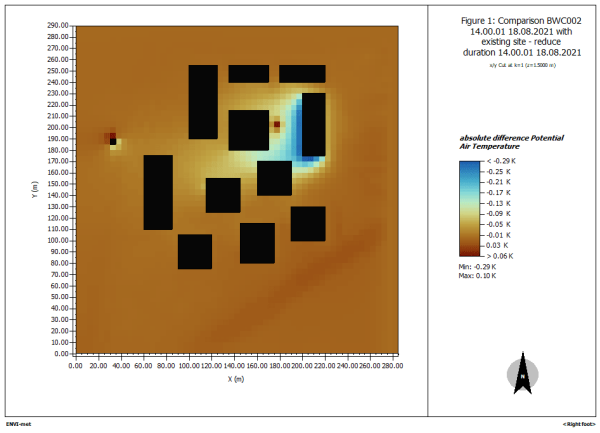

Figure 66: Relative Humidity Changes with Building materials changes - 14h

It can be easily observed than the change in Relative Humidity over the site is close to 0 despite the added water bodies. The effect of the pound is unnoticeable by any change of RH, while fountains bring effective, but very local effect, adding up to 5.3 % RH where they are, what explain the as well local effect of cooling previously observed. As for the building material changes, they don't bring significant improvement of the Site RH, those changes being close to 0 %. The single green façade improves by 0.3 % at most the RH close to it.

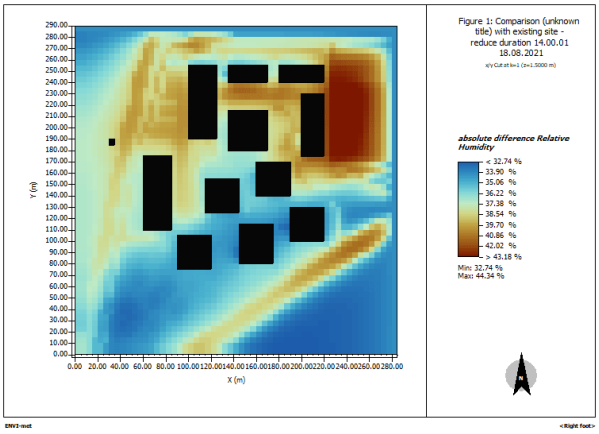

Figure 67: Relative humidity change with vegetation extension - 14h

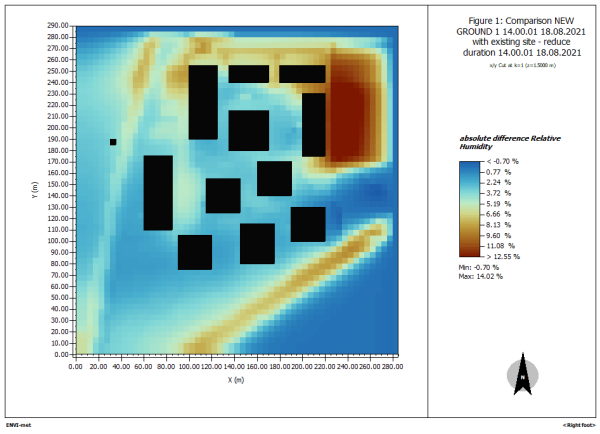

Figure 68: Relative Humidity Changes with Building materials changes - 14h

The new ground as well as the added vegetation lead to overall higher RH rates on the whole site, what can explain the observed overall cooling effects this two measures, again, the two most effective out of the 4 explored, have on the site.

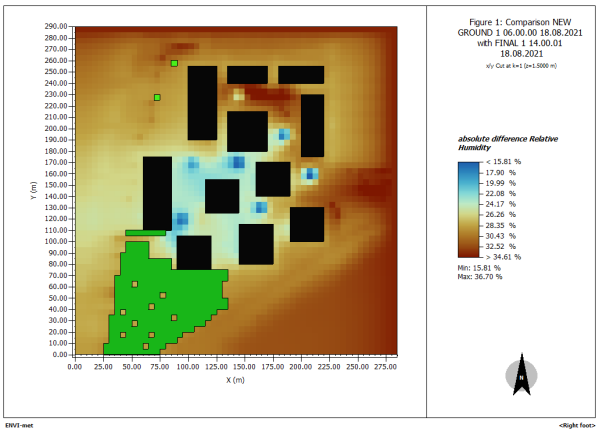

Figure 69: RH changes with ground change versus integrated solutions - 14h

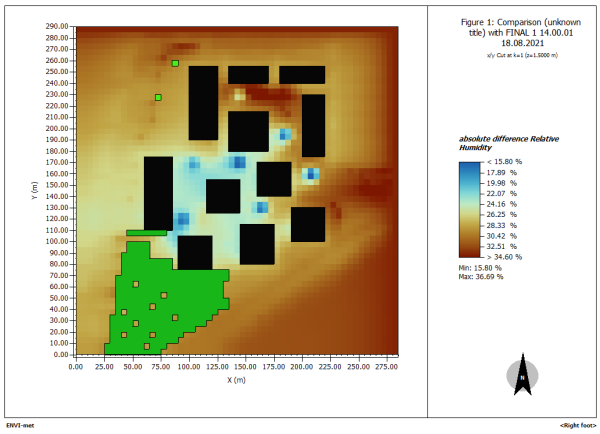

Figure 70: RH changes with extended vegetation versus integrated solutions - 14h

As for temperatures comparison, both vegetation and ground changes affect the site in very similar ways compared to the final integrated solutions. Mixing solutions together brings more relative humidity up to 34.6 %, and positive changes can be noticed all over the site.

4.2.3 Changes in Heat fluxes

For comparing easier the different base cases, the energetical aspect will be analyzed thanks to the latent and sensible heat fluxes, both displayed for each base case here below.

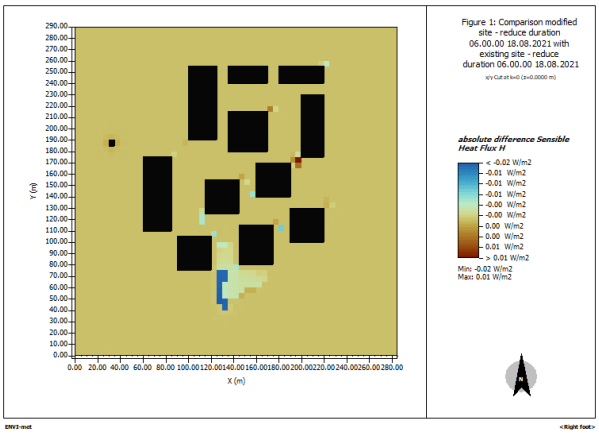

Figure 71: Compared sensible heat fluxes - 14h

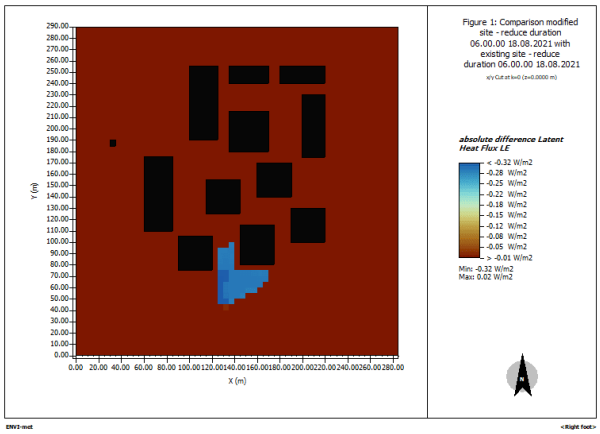

Figure 72: Compared latent heat fluxes - 14h

Adding water bodies made negligible changes in both heat fluxes, close to 0 W/m^2. The single place that can be distinguished is the pond, that gives up a little bit more heat flux, but the maximum of 0.32 W/m^2 is negligible too compared to the scale of 100 W/m^2 that are observed on the site. However, when combined to the others solutions, it can be observed that it induces more humidity around the water bodies on wider areas of influence.

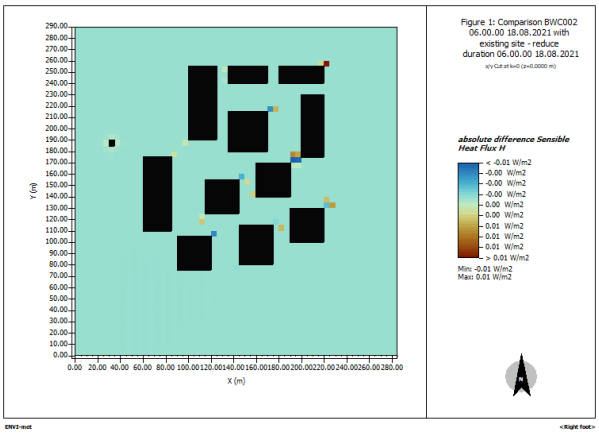

Figure 73: Compared sensible heat fluxes, new building materials - 14h

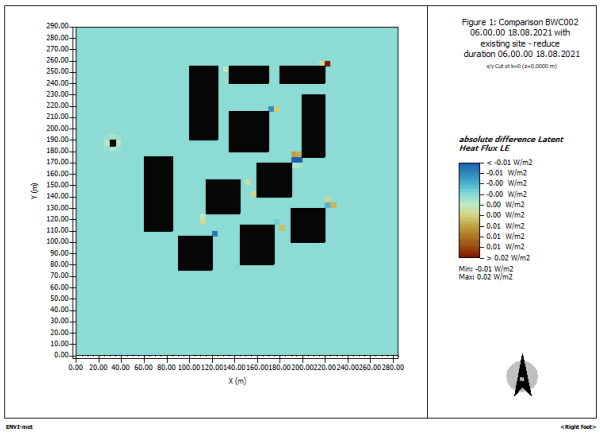

Figure 74: Compared latent heat fluxes, new building materials - 14h

Building new material, similarly as in the case of water bodies, introduce almost no change in the heat fluxes.

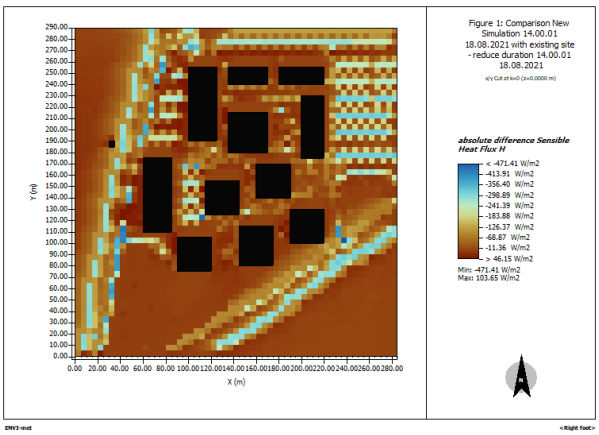

Figure 75: Compared sensible heat fluxes, added vegetation - 14h

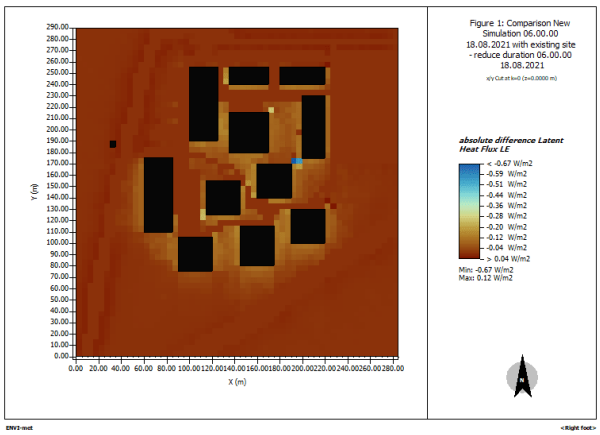

Figure 76: Compared latent heat fluxes, added vegetation - 14h

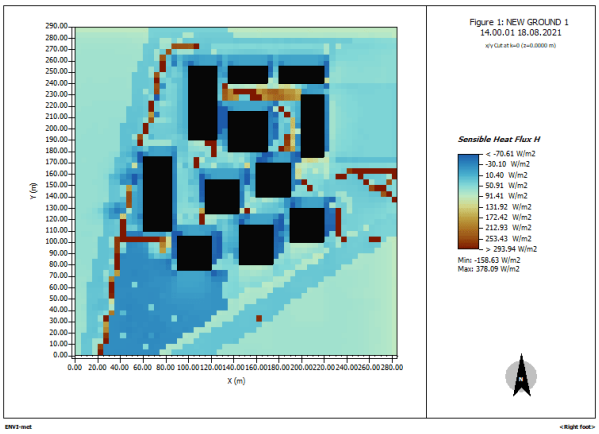

Figure 77: Compared sensible heat fluxes, new ground - 14h

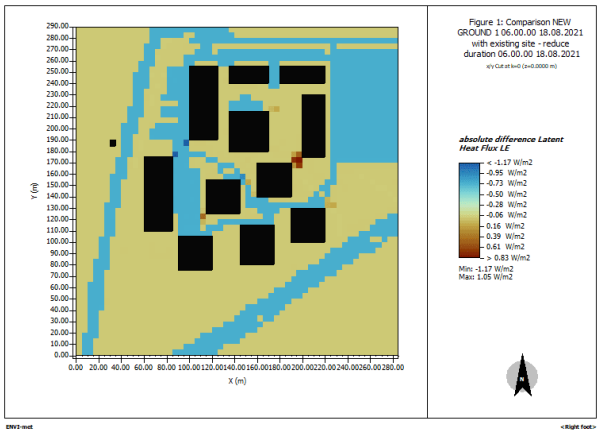

Figure 78: Compared latent heat fluxes, new ground - 14h

On the contrary to the two first studied cases, adding vegetation and changing the ground composition impacts a lot the heat fluxes that can be observed. After the ground change, even if at some rare points the ground emitts up to

293.9 W/m^2 more, it also can be observed that one fourth of surfaces are releasing less sensible heat. Still, the brought changes are producing very variate effects as different materials were used. As for the extension of the vegetation, the latent heat fluxes from ground to air are very slightly diminished, up to -0.67 W/m^2. The real changes are brought to the sensible heat fluxes, that are reduced up to 471.4 W/m^2, what can be explained by the protection from solar radiation brought by the vegetation. The latent heat fluxes that are not showed are those occurring at the level of the vegetation by evaporative cooling allowed by the water vapour released by the evapo-transpiration of plants.

I think the reason for such low latent heat flux is due to the height of the visualisation. You set k =0, maybe at crown height there is more change.

4.2.4 Comparing base cases : Overview

As seen previously, the strategies that improve the most the Innovation Park microclimate conditions are the ground change and the extension of greenings. Both have a really positive global effect, reducing temperatures all over the site down to 3.1 and 3.2 °C at some points, respectively. The water bodies implementation does not have more than local improvement effects, for both humidity and air temperature, but still can provide, all the day long except for the mid-afternoon, cooler points for resting outdoors.

4.3 Outcome of the Integrated Microclimate Solution

4.3.1 Potential Air Temperature

The integrated microclimate solution significantly reduced potential air temperatures across the EPFL Innovation Park. The bottom figures 79 illustrate the potential air temperature at 14h for the base case, the integrated solutions case, and the absolute differences. On average, a cooling effect of 2.5–3°C was observed, with localized reductions reaching up to 5°C. Central courtyards, represented by the strongest blue zones, experienced the greatest cooling (up to 5°C) due to the combined effects of fountains, vegetation, and green roofs. The top-right parking lot transitioned from dark brown to white, showing a notable temperature reduction of 3–4°C, attributed to the use of porous asphalt and grass. The main roads on the left also saw a similar cooling effect of 3–4°C, while the bottom roads experienced a milder reduction of about 2.4°C, driven primarily by the shading effect of large-canopy trees. These temperature reductions highlight the effectiveness of the integrated strategies in mitigating the urban heat island (UHI) effect.

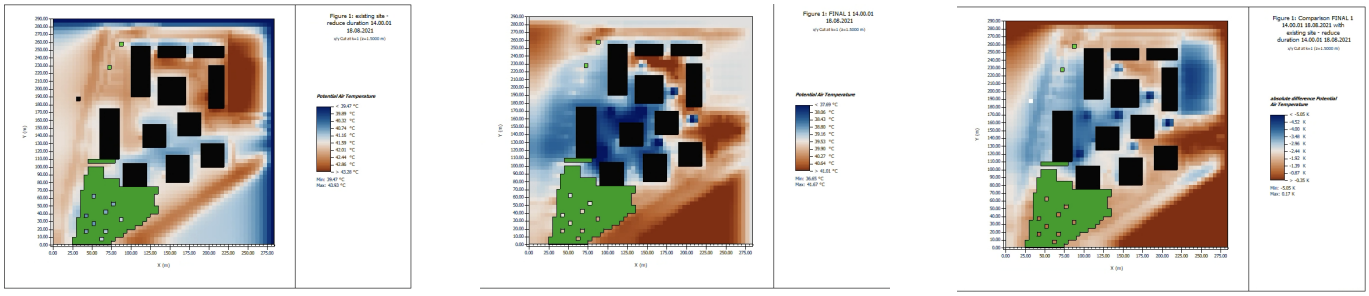

(a) Base Case (b) Integrated Solution (c) Absolute Difference

Figure 79: Potential air temperature at 14h: (a) Base Case, (b) Integrated Solution, and (c) Absolute Difference.

4.3.2 Relative Humidity and Wind Speed

Our integrated microclimate solution significantly influenced relative humidity (RH) across the EPFL Innovation Park, with increases ranging from -1.03% to 29.47%. The fountains surrounding areas, marked by brown and red zones and central courtyards, showed the greatest RH increases (14–29%), mainly due to the addition of fountains and enhanced evapotranspiration from vegetation. Meanwhile, main roads and parking lots experienced RH changes (5-14%), thanks to nearby street trees and porous asphalt. This is a positive outcome, as increased RH enhances thermal comfort through better latent heat flux and moisture retention.

Only minor wind speed changes are observed. The perimeters of Cluster B buildings experienced a slight increase in wind speed of about 0.15 m/s, which could improve natural ventilation. Overall, the integrated microclimate solutions have little impact on wind speed.

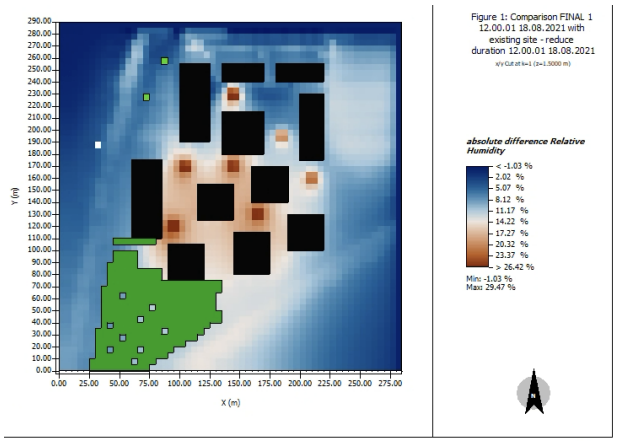

(a) Absolute difference in relative humidity at 14h.

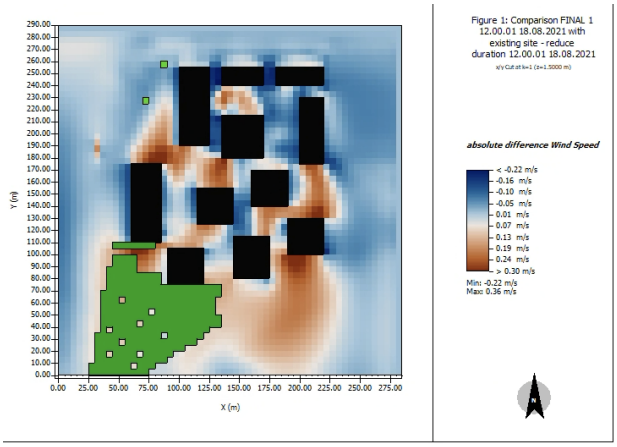

(b) Absolute difference in wind speed at 14h.

Figure 80: (a) Absolute difference in relative humidity and (b) Absolute difference in wind speed at 14h, shown side by side for comparison.

4.3.3 Soil Temperature

The integrated microclimate solution achieves substantial soil temperature reductions across the EPFL Innovation Park, with differences ranging from -18.99 K (maximum cooling in dark blue zones) to +15.28 K (anomalous red dots likely due to modelling errors). The main roads and left and right parking lots have the greatest cooling, with reductions from 12 to 18.99 K, primarily due to reflective and permeable ground materials mitigating heat absorption. In the central area, moderate reductions (light blue, around -5 K to -8 K) are observed, mainly resulting from enhanced vegetation improving shading and evapotranspiration. Overall, the solution demonstrates exceptional soil cooling in high-impact zones while maintaining improved microclimate conditions across the site.

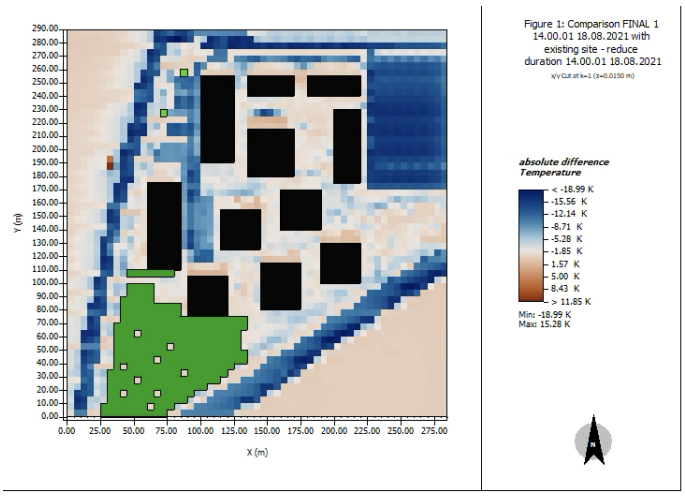

Figure 81: Absolute difference in Soil Temperature at 14h.

4.3.4 Surface Heat Flux

The integrated heat flux dynamics reveal significant changes in energy balance, primarily in roads and car parks. Surface latent heat flux (LE) increases by up to +721 W/m^2 in these areas due to enhanced evapotranspiration from newly planted street trees and denser grass coverage, while reductions beneath tree canopies indicate a shift in cooling from soil evaporation to canopy transpiration. Sensible heat flux (H) decreases by as much as 411 W/m^2, and ground heat flux (G) reduces by up to 490 W/m^2, reflecting the effectiveness of porous and reflective materials and vegetation in limiting heat absorption and reducing heat transfer to the air.

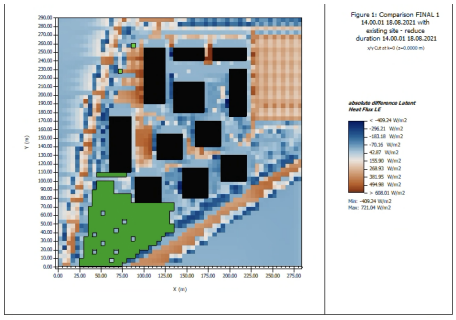

Figure 82: Latent Heat Flux.

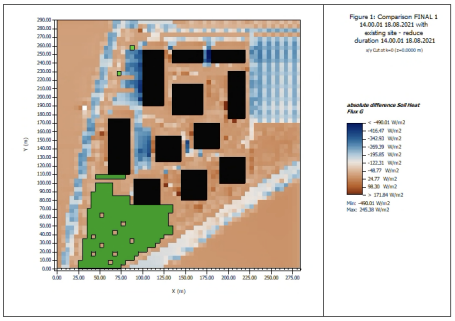

Figure 83: Ground Heat Flux.

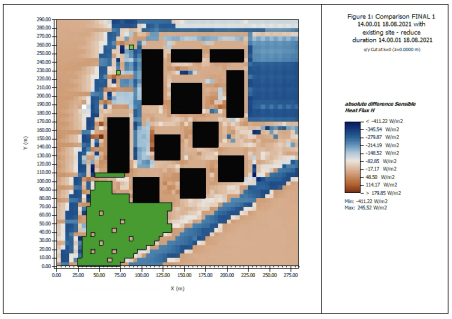

Figure 84: Sensible Heat Flux.

4.3.5 Wall and Roof Temperatures, Sensible and Latent Heat Flux of the Building

Roof temperatures show the largest reductions of impressive 39°C to 49.72°C (blue zones). Thanks to the newly added roof greenings, which help to effectively insulate the buildings and reduce solar heat absorption. In comparison, the southwest corner building without green roofs (our modeling mistake) exhibits negligible cooling.

Figure 79(a) also illustrated that Building Block C, which previously had overheated walls, experienced the most notable wall temperature drop of 15–20°C thanks to added wood panelling insulation. Surprisingly, we discovered that Building Block B, even without wall material interventions, also showed substantial wall temperature reductions of about 12°C in every direction. We believe that our integrated solutions are contributing to this exciting indirect cooling effect, potentially because of denser street trees surrounded by cooler roofs and increased moisture from fountains. In Building Block A, a slight temperature decrease of about 5°C was observed on the south-facing walls, with only minor changes in other directions. While the temperature drop is not as pronounced as in Building Block B, this result is still promising. It suggests that our integrated solutions helped to mitigate the mild overheating issues in the base case for this wall, even without implementing any material changes or facade greening interventions.

Roofs show substantial reductions in sensible heat flux, with values as low as -542.21 W/m^2, primarily due to green roofs providing insulation and reducing solar heat absorption, while latent heat flux increases up to +135.54 W/m^2 are driven by enhanced evapotranspiration from vegetation. Walls of Building Block B experienced sensible heat flux reductions of 40–130 W/m^2, which coincide with the surprising wall temperature drops. Block C showed similar reductions in sensible heat flux on its south and west walls, while minimal reductions or slight increases were observed on its north and east walls and Block A.

Our analysis revealed surprising and unexpected results on top of the expected ones, showcasing how the interplay of various mitigation strategies can produce remarkable outcomes in urban microclimate management and also tested the effectiveness of our integrated solutions.

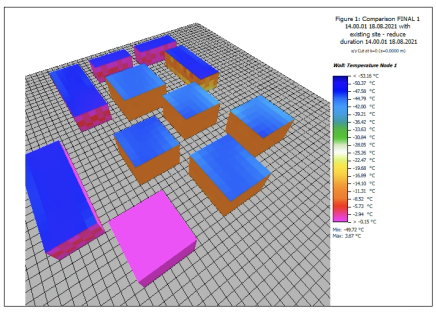

(a) Absolute difference of wall temperature at 14h.

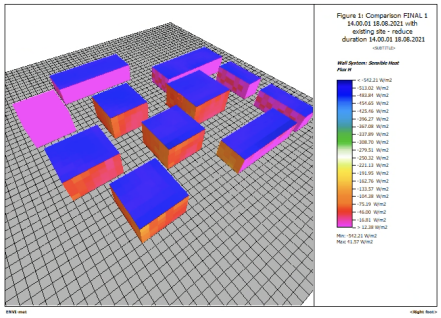

(b) Absolute difference of wall system sensible heat flux at 14h.

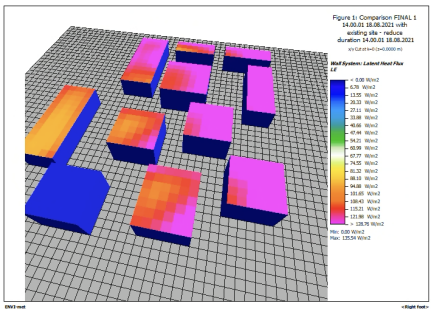

(c) Absolute difference of wall system latent heat flux at 14h.

Figure 85: Comparison of wall temperature, sensible heat flux, and latent heat flux differences across the building blocks.

4.3.6 PET (Physiological Equivalent Temperature)

PET quantifies the combined effects of air temperature, mean radiant temperature (MRT), wind speed, and humidity on human thermal comfort. In the base case, PET values exceed 58°C across most of the site, with cooler areas restricted to the north and east boundaries of buildings. In the final case, cooler zones extend to inner lanes, main roads, and car parks, reducing values to below 47°C in many areas. PET reductions reach up to -13.06°C, driven

by interventions such as street trees, green roofs, and reflective materials, which collectively transform previously heat-stressed areas into thermally comfortable zones.

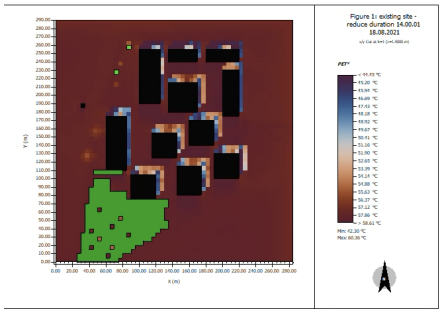

Figure 86: PET values in the base case at 14h.

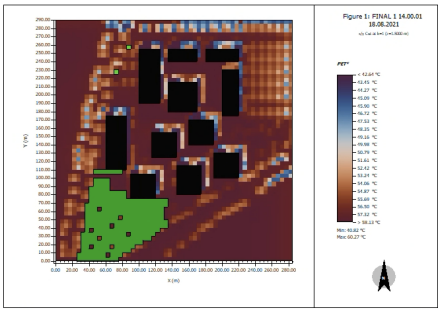

Figure 87: PET values in the final case at 14h.

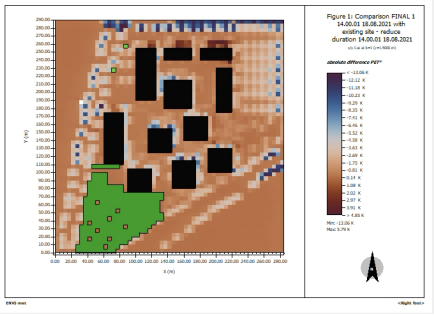

Figure 88: Absolute difference in PET at 14h.

4.3.7 MRT (Mean Radiant Temperature)

MRT measures radiative heat exchange between a person and surrounding surfaces. In the base case, MRT values exceed 60°C in open areas like roads, car parks, and inner lanes, with cooling limited to shaded building perimeters. In the final case, MRT reductions of up to -27.21 K are observed, particularly in vegetated zones, shaded pathways, and reflective ground surfaces. These improvements align closely with PET reductions, validating the effectiveness of shading, vegetation, and reflective materials in mitigating radiative heat stress.

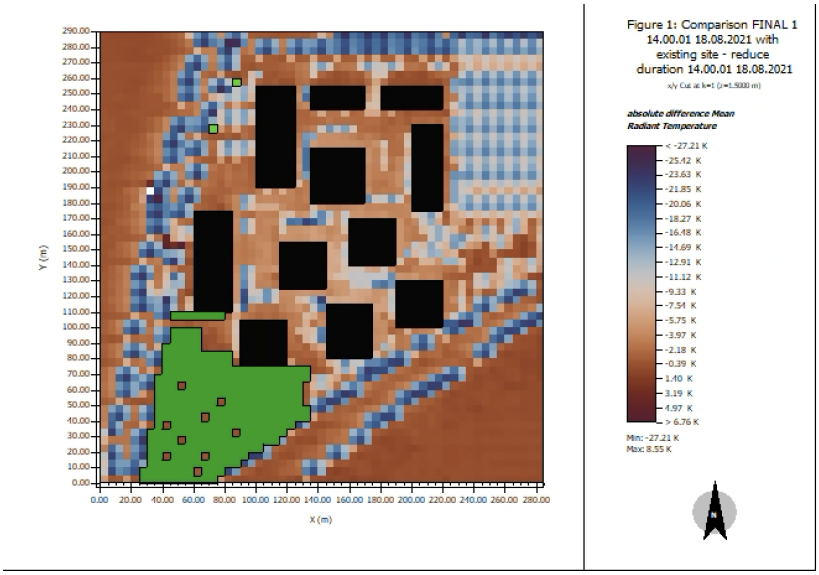

Figure 89: Absolute difference in MRT at 14h.

4.3.8 Outcome

Overall, by comparing key environmental parameters and outdoor thermal comfort indices, our findings confirm that the integrated microclimate solution is efficient in mitigating Urban Heat Island effects, enhancing microclimatic conditions, and promoting thermal comfort across EPFL innovation park.

5 Conclusion

The EPFL Innovation Park faces significant urban microclimate challenges, primarily driven by the Urban Heat Island (UHI) effect. These challenges stem from high solar radiation absorption, heat retention by impervious surfaces, limited vegetation, and unoptimized building materials. Through an analysis using ENVI-met simulations, this project identified critical areas of thermal stress and proposed different mitigation strategies.

The findings underscore the importance of vegetation, which emerged as the most effective solution in terms of urban microclimate as well as ecologically. Strategic implementations, such as tree-lined streets, green roofs, and denser greenery, significantly reduced surface temperatures by up to 40°C and localized air temperatures up to 3.6°C. Green roofs provided insulation and evapotranspiration benefits, while shaded streets improved pedestrian comfort. In

contrary, green facades were less effective for buildings with high thermal mass but performed well on lightweight materials.

Ground modifications, including porous asphalt and reflective coatings, contributed to a quite uniform temperature reduction, particularly in parking lots and roads, by decreasing heat absorption and enhancing latent heat transfer. Although water bodies have limited spatial cooling effects, their inclusion improved localized thermal comfort and create inviting rest areas for work breaks in summer.

Overall, the integration of vegetation, ground changes, and water features into urban design present a feasible pathway to mitigate UHI effects and improve thermal comfort at EPFL Innovation Park. By implementing these strategies, the site can achieve better sustainability, reduced energy demand, and improved work environment quality for its users.

As well as the implemented solutions performed, they are by far not the only ones applicable: Solutions implemented in cities are for example hanging parasols and sheets over the open streets between buildings. A further Improvement of the urban Microclimate could be achieved, by expanding the sustainability policy over a larger area, as vegetation has a only local effect ; it's urban penetration can be improved by increasing the area where it is applied, as well as a good distribution of the vegetation effect. This might be implemented on the whole campus, as a further improvement.

6 Annexes

Properties	Units	EPS Insulation[1]	Plywood (heavyweight)[2]	Gravel[3]	XPS Insulation[4]	Fiber cement board[5]	Sandwich panel mineral wool[6]	Mineral wool insulation[7]	EPS+Concrete[8]
Absorption	%	0.3	0.42	0.7	0.3	0.7			0.3
Transmission	%	0	0.13	0	0	0			0
Reflection	%	0.7	0.45	0.3	0.7	0.3			0.7
Emissivity	%	0.9	0.9	0.94	0.9	0.94			0.9
Specific Heat	J/kgK	1.053	0.643	16.25	0.714	1.126	0.190	0.154	0.921
Thermal Conductivity	W/mK	0.03	0.022	0.4	0.024	0.216	0.039	0.04	1.27
Density	kg/m3	19	700	80	28	1350	105	130	1945

Figure 90: Material Properties as inputted to ENVI-met. References Below

- 1:[1] & [18]
- 2:[1] & [19]
- 3:[1] & [20]
- 4:[1] & [22]
- 5:[1] & [21]
- 6:[1]
- 7:[1] & [23]
- 8:[1]

Table 2: Tree Types and Characteristics

Tree Type	**Height (m)**	**Placement**
London Plane	20–25	Along major roads
Field Maple	10–15	Rows and perimeters of parking lots
Small-leaved Lime	15–20	Along narrower pathways and pedestrian lanes

Table 3: Green Roofs Parameters

Parameter	**Extensive Green Roof**	**Intensive Green Roof**	**Lightweight Green Roof**
Plant Type	Grass 25 cm dense	Grass 50 cm dense / Funkia	Fern
Plant Thickness (m)	0.25	0.5 / 3.0	0.1–0.15
LAI	2.5	4.0	2.0
LAD	0.3	0.5 / 0.4	0.7
Substrate Type	Silt Loam (SO)	Loam (LE), Sandy Loam (SL)	Sandy Loam (SL), Sand (SD)
Thickness (m)	0.1	0.2 + 0.05	0.08 + 0.05
Emissivity	0.95	0.94	0.91
Albedo	0.2	0.22	0.23
Water Coefficient	0.4	0.46	0.34
Air Gap (m)	None	None	0.05

Table 4: Green Facades Parameters

Parameter	Concrete Facades	Fiber Cement Facades	Aluminum Facades
Plant Type	Ivy	Funkia	Ivy
Plant Thickness (m)	0.3	0.2	0.15–0.2 / 3.0
LAI	4.5	3.5	2.5–3.0
LAD	0.3	0.4	0.5
Substrate Type	Loam (LE)	Sandy Clay Loam (TS)	Sandy Loam (SL)
Thickness (m)	0.2	0.15	0.1
Emissivity	0.95	0.9	0.85
Albedo	0.2	0.25	0.3
Water Coefficient	0.45	0.3	0.2
Air Gap (m)	0.05	0.05	0.05

7 References

[1] CIVIL-309 Lecture Notes - Urban Thermodynamics - Assist. Prof. Doolana Khovalyg

[2] EPFL Logo:
https://inside.epfl.ch/corp-id/logo-fichiers/

[3] https://www.fhwa.dot.gov/pavement/asphalt/pubs/hif15009.pdf

[4] https://en.wikipedia.org/wiki/Pervious_concrete

[5] Yinghong Qin, A review on the development of cool pavements to mitigate urban heat island effect, Renewable and Sustainable Energy Reviews, Volume 52, 2015, Pages 445-459, ISSN 1364-0321, https://doi.org/10.1016/j.rser.2015.07.177.

[6] S. Tsoka, T. Theodosiou, K. Tsikaloudaki, F. Flourentzou, Modeling the performance of cool pavements and the effect of their aging on outdoor surface and air temperatures, Sustainable Cities and Society, Volume 42,2018,Pages 276-288,ISSN 2210-6707, https://doi.org/10.1016/j.scs.2018.07.016.

[7] https://www.persee.fr/doc/globe_0398-3412_1962_num_102_1_3490#:~:text=Ainsi%2C%20tout%20autour%20du%20LÃl'man,et%20maximum%20Ãă%20l'automne.

[8] Syafii, N.I., Ichinose, M., Kumakura, E., Jusuf, S.K., Hien, W.N., Chigusa, K., Ashie, Y., 2021. Assessment of the Water Pond Cooling Effect on Urban Microclimate: A Parametric Study with Numerical Modeling. International Journal of Technology. Volume 12(3), pp. 461-471. https://doi.org/10.14716/ijtech.v12i3.4126

[9] S. Bouketta, Urban Cool Island as a sustainable passive cooling strategy of urban spaces under summer conditions in Mediterranean climate, Sustainable Cities and Society, Volume 99, 2023, 104956, ISSN 2210-6707, https://doi.org/10.1016/j.scs.2023.104956.

[10] Lei Tang, Weimin Zheng, Yulin Wu, Li Tang, Yuhu Zhao, Evaluating the cooling performance of vegetation combined with a fountain in horizontal and vertical urban environments, Building and Environment, Volume 267, Part B, 2025, 112192, ISSN 0360-1323, https://doi.org/10.1016/j.buildenv.2024.112192. (https://www.sciencedirect.com/science/article/pii/S0360132324010345)

[11] Balany, F.; Muttil, N.; Muthukumaran, S.; Wong, M.S.; Ng, A.W.M. Studying the Effect of Blue-Green Infrastructure on Microclimate and Human Thermal Comfort in Melbourne's Central Business District. Sustainability 2022, 14, 9057. https://doi.org/10.3390/su14159057

[12] Bowler, D. E., Buyung-Ali, L., Knight, T. M., Pullin, A. S. (2010). Urban greening to cool towns and cities: A systematic review of the empirical evidence. *Landscape and Urban Planning, 97*(3), 147–155. https://doi.org/10.1016/j.landurbplan.2010.05.006.

[13] Souch, C. A., Souch, C. (1993). The effect of trees on summertime below-canopy urban climates: A case study Bloomington, Indiana. *Journal of Arboriculture, 19*(5), 303–312.

[14] Santamouris, M. (2014). Cooling the cities–A review of reflective and green roof mitigation technologies to fight heat island and improve comfort in urban environments. *Solar Energy, 103*, 682–703. https://doi.org/10.1016/j.solener.2012.07.003.

[15] Perini, K., Magliocco, A. (2014). Effects of vegetation, urban design, and design strategies on outdoor thermal comfort. *Building and Environment, 44*(1), 81–90. https://doi.org/10.1016/j.buildenv.2014.01.007.

[16] Yoshida, A., Shoho, S., Kinoshita, S., (2017) Evaluation of reduction effect on thermal load inside and outside of concrete building with wooden decoration by numerical analysis. *Energy Procedia, Volume 132, 435-440.* https://doi.org/10.1016/j.egypro.2017.09.653.

[17] Moretti, E., Belloni, E., Agosti, F., (2016). Innovative mineral fiber insulation panels for buildings: Thermal and acoustic characterization. *Applied Energy, Volume 169, 421-432* https://doi.org/10.1016/j.apenergy.2016.02.048.

[18] Jablite HP+ External Wall Insulation Board, *Renders Direct, accessed 13/11/2024*, https://rendersdirect.co.uk/products/jablite-hp-external-wall-insulation-board-1200-x-600-x-50mm

[19] PIR-Plywood Laminate Insulation Board, *insulation4less, accessed 13/11/2024*, https://insulation4less.co.uk/products/pir-plywood-laminate-insulation-board-all-sizes

[20] Gravel Ballasted Roofs, *Sika Group, accessed 13/11/2024*, https://www.sika.com/en/construction/roof-systems/gravel-ballasted-roofs.html

[21] "Hocreboard" Fiber cement board, *HBD, accessed 13/11/2024*, https://hocre-board.com/products/fiber-cement-board/#:~:text=In%20addition%20to%20being%20a,it%20a%20superior%20Heat%20Insulator.

[22] XPS (Extruded Polystyrene or Styrofoam), *ixl, accessed 13/11/2024*, https://www.ixl.co.th/en/products/ixl-insulated-panel/xps-extruded-polystyrene-or-styrofoam/#:~:text=XPS%20(Extruded%20Polystyrene%20or%20Styrofoam)%20has%20a%20standard%20density%20of,50%20to%2075%20degrees%20Celsius

[23] ARPANEL S MiWo wall sandwich panels – standard fastening system, *ARPANEL, accessed 14/11/2024*, https://arpanel.eu/products/miwo/miwo-wall-sandwich-panels/#produkt-1